
HETEROGENEOUS REACTORS

The kinetics and reactor designs we have considered thus far are for homogeneous reactions. The remainder of the book is devoted to heterogeneous reactions. Many systems are heterogeneous because a catalyst is necessary, and this substance is commonly (but not always) in a phase different from that of the reactants and products. Accordingly, our first objective will be a study (Chaps. 8 and 9) of heterogeneous catalysis and kinetics of heterogeneous catalytic reactions.

The fact that phase boundaries are inherent in heterogeneous systems introduces the need to deal with physical processes (mass and energy transfer) between the bulk fluid and the catalyst. Thus physical processes affect reactor design in a more intrinsic way for heterogeneous reactions than for homogeneous ones. It is common practice to write mass and energy balances for heterogeneous and homogeneous systems in the same way; e.g., as given in Chap. 3. When this is done, the rate equation used for heterogeneous systems will include the effects of physical processes.

To illustrate, in Eq. (3-1) the rate is expressed per unit volume. If the volume element includes a heterogeneous mixture of reaction fluid and solid catalyst particles, the proper rate to use in Eq. (3-1) will include

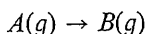
the effects of mass- and energy-transfer processes from fluid to solid surface and within the solid particle. Such rates are sometimes called *global*, or *overall*, rates of reaction. The advantage of using the global rate is that the design equations for heterogeneous systems are identical to those for homogeneous systems, as presented in Chaps. 3 to 5. However, expressions for the global reaction rate must be formulated in terms of properties of the bulk fluid. This is accomplished by writing expressions for the rate of each step in the overall process. The sequence of steps for converting reactants to products is as follows:

1. Transport of reactants from the bulk fluid to the fluid-solid interface (external surface of catalyst particle)
2. Intraparticle transport of reactants into the catalyst particle (if it is porous)
3. Adsorption of reactants at interior sites of the catalyst particle
4. Chemical reaction of adsorbed reactants to adsorbed products (surface reaction)
5. Desorption of adsorbed products
6. Transport of products from the interior sites to the outer surface of the catalyst particle
7. Transport of products from the fluid-solid interface into the bulk-fluid stream

At steady state the rates of the individual steps will be identical. This equality can be used to develop a global rate equation in terms of the concentrations and temperatures of the bulk fluid. The derivation of such equations will be considered in detail in Chaps. 10 to 12, but a very simple treatment is given next to illustrate the nature of the problem.

7-1 Global Rates of Reaction

Consider an irreversible gas-phase reaction



which requires a solid catalyst C . Suppose that the temperature is constant and that the reaction is carried out by passing the gas over a bed of *non-porous* particles of C . Since the catalyst is nonporous, steps 2 and 6 are not involved. The problem is to formulate the rate of reaction per unit volume¹

¹As defined, the volume element on which r_v is based must include at least one catalyst particle; otherwise the interphase physical effects cannot be considered. Yet this rate is used in Eqs. (3-1) and (3-2) as a rate applicable to a differential volume, i.e., as a point rate. This is an approximation which arises from treating the discrete nature of a bed of catalyst particles

of the bed—that is, the *global rate for a catalyst particle*, r_p —in terms of the temperature and concentration of A in the bulk-gas stream. Note that these are the quantities that are measurable or can be specified (as design requirements), rather than the temperature and concentration at the gas-particle interface. Global rates of catalytic reactions are usually expressed per unit mass of catalyst, i.e., as r_p . These are easily converted to rates per unit volume by multiplying them by the bulk density ρ of the bed of catalyst particles.

The overall conversion of A to B in the bulk gas occurs according to steps 1, 3 to 5, and 7 in series. Let us further simplify the problem by supposing that steps 3 to 5 may be represented by a single first-order rate equation. Then the overall reaction process may be described in three steps: gas A is transported from the bulk gas to the solid surface, the reaction occurs at the interface, and finally, product B is transported from the catalyst surface to the bulk gas. Since the reaction is irreversible, the concentration of B at the catalyst surface does not influence the rate. This means that r_p can be formulated by considering only the first two steps involving A . Since the rates of these two steps will be the same at steady state, the disappearance of A can be expressed in two ways: either as the rate of transport of A to the catalyst surface,

$$r_p = k_m a_m (C_b - C_s) \quad (7-1)$$

or as the rate of reaction at the catalyst surface,

$$r_p = k a_m C_s \quad (7-2)$$

In Eq. (7-1) k_m is the usual mass-transfer coefficient based on a unit of transfer surface, i.e., a unit of external area of the catalyst particle. In order to express the rate per unit mass¹ of catalyst, we multiply k_m by the external area per unit mass, a_m . In Eq. (7-2) k is the *reaction-rate constant* per unit surface. Since a positive concentration difference between bulk gas and solid surface is necessary to transport A to the catalyst, the surface concentration C_s will be less than the bulk-gas concentration C_b . Hence Eq. (7-2) shows that the rate is less than it would be for $C_s = C_b$. Here the effect of the mass-transfer resistance is to reduce the rate. Figure 7-1 shows schematically how the concentration varies between bulk gas and catalyst surface.

as a continuum. It is a necessary approximation because it is not yet possible to take into account variations in heat- and mass-transfer coefficients with position on the surface of a single catalyst particle. Thus average values of these coefficients over the particle surface are employed in formulating global rates. This is the value denoted by k_m in Eq. (7-1).

¹Instead of rate per unit mass of catalyst, Eqs. (7-1) and (7-2) could be expressed as rates per unit external surface, in which case a_m would not be needed in Eq. (7-1). Alternately, a rate per particle could be used. We shall generally use the rate per unit mass.

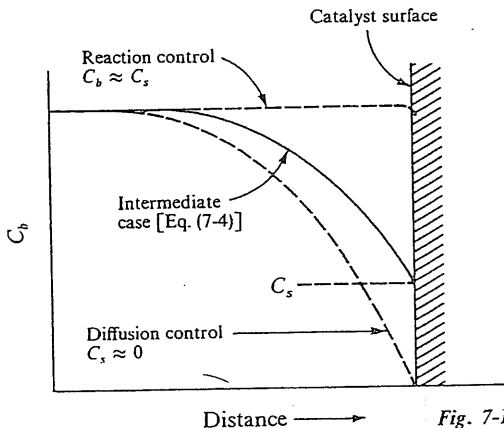


Fig. 7-1 Mass transfer between fluid and catalyst surface

The global rate can be expressed in terms of C_b by first solving for C_s from Eqs. (7-1) and (7-2); thus

$$C_s = \frac{k_m}{k_m + k} C_b \quad (7-3)$$

Then this result is substituted in either Eq. (7-1) or Eq. (7-2) to give

$$r_p = \frac{kk_m a_m}{k_m + k} C_b = \frac{a_m}{1/k + 1/k_m} C_b \quad (7-4)$$

This is the expression for the global rate in terms of the bulk-reactant concentration. The concentration profile in this case is shown by the solid line in Fig. 7-1. It is a very restricted illustration of a global rate, since heat-transfer resistances were not considered (constant temperature was assumed) and only external mass transfer is involved (the catalyst particle is nonporous). These restrictions are removed in the detailed treatment in Chaps. 10 and 11, but this simple example illustrates the meaning of global rates of reaction for heterogeneous systems.

A hypothetical reaction has been used to develop the previous results. It is of interest to know the magnitude of the global rate for real situations. Fortunately, considerable experimental data are available. Measurements¹ for the oxidation of SO_2 with air on a platinum catalyst, deposited on $1/8 \times 1/8$ -in. cylindrical pellets,² gave a global rate of 0.0956 g mole/(hr)(g catalyst). The bulk temperature of the gas was 465°C and the gas velocity in the catalyst bed was 350 lb/(hr) (ft²). The bulk composition corresponded to a 10% con-

¹R. W. Olson, R. W. Schuler, and J. M. Smith, *Chem. Eng. Progr.*, **42**, 614 (1950).

²The particles were of porous alumina, but the platinum was deposited on the outer surface, so that, in effect, a nonporous catalyst was used.

version of a 6.5 mole % SO_2 -93.5% air mixture. At these conditions both mass- and heat-transfer resistances between the bulk gas and the surface of the catalyst pellets were important. Calculations with Eq. (7-1) indicated that the partial pressure of SO_2 dropped to 0.040 atm at the solid surface from the value of 0.06 atm in the bulk gas. This relatively large difference means that the diffusion resistance was large. If the rate were evaluated without consideration of this resistance—that is, if it were evaluated for $p_{\text{SO}_2} = 0.06$ atm at 465°C —it would be 0.333 g moles SO_2 reacted/(hr) (g catalyst). At $p_{\text{SO}_2} = 0.04$ atm it would be 0.0730. Hence the error in neglecting the mass-transfer resistance would be large; that is, the rate so computed would be $(0.333/0.0730)$ (100), or 350% higher than the global rate.

Actually, the temperature at the catalyst surface is about 15°C above the bulk-gas temperature (see Example 10-2) because of heat-transfer resistance. Hence the reaction at the catalyst surface occurred at 480°C . According to the activation energy for this reaction, a 15°C temperature rise would increase the rate about 31%. Hence neglecting the heat-transfer resistance leads to a rate 31% less than the global value. If both thermal and diffusion resistances were neglected, the rate would be $(0.333/0.0956)$ (100), or 250% higher than the global rate. For this exothermic reaction the diffusion and thermal resistances have opposite effects on the rate. The example is extreme in that mass-transfer resistance was relatively large in comparison with reaction resistance. At lower temperatures and/or higher gas velocities past the catalyst pellet (higher k_m) the mass-transfer effect would be less.

Frequently heat-transfer resistances are much larger than mass-transfer resistances, in contrast to the preceding example. As an illustration, consider the data of Maymo and Smith¹ for the oxidation of hydrogen with oxygen on a platinum-on-alumina catalyst. Rates and temperatures were measured for a single porous catalyst pellet (1.86 cm diameter) suspended in a well-mixed gas containing primarily hydrogen with a small percentage of oxygen and water vapor. Because of the turbulence in the gas, the concentration difference between bulk gas and pellet surface was negligible. However, there was a significant thermal resistance, so that the pellet-surface temperature was greater than the bulk-gas temperature. The pellet was porous with uniform distribution of platinum throughout. Hence there were internal resistances, both to mass and to heat transfer. In one particular run the measured rate of water production was 49.8×10^{-6} mole/(g catalyst) (sec). This is the global value and includes the effects of both internal and external physical resistances. The bulk-gas, pellet-surface, and pellet-center temperatures were 89.9, 101, and 147.7°C , respectively. The rate of the chemical step on the surface was also measured by experiments with fine particles of catalyst for which there were no temperature or concentration differences between bulk

¹J. A. Maymo and J. M. Smith, *AIChE J.*, 12, 845 (1966).

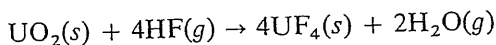
gas and surface or interior of particle. This intrinsic rate was correlated by the equation

$$r = 0.655 p_{O_2}^{0.804} e^{-5,230/R_g T} \quad (7-5)$$

where p is in atmospheres and T is in degrees Kelvin. We can evaluate the effect of the external resistance in the following way. First calculate the rate at the surface temperature ($101 + 273^\circ\text{K}$) and $p_{O_2} = 0.0527$ atm, which is the oxygen partial pressure, either in the bulk gas or at the pellet surface. Substituting these quantities in Eq. (7-5) gives $r = 54.3 \times 10^{-6}$ mole/(g catalyst)(sec). If the rate were evaluated at bulk-gas conditions (89.9°C and $p_{O_2} = 0.0527$ atm), the result from Eq. (7-5) would be 43.6×10^{-6} mole/(g catalyst) (sec). Hence neglecting the external-temperature difference would give a rate $[(54.3 - 43.6)/54.3]$ (100), or 20%, less than the correct value.

This example also shows the effects of mass- and energy-transfer resistances within the catalyst pellet. The temperature increases toward the center of the pellet and increases the rate, but the oxygen concentration goes down, tending to reduce the rate. The global value of 49.8×10^{-6} is the resultant balance of both factors. Hence the net error in using the bulk conditions to evaluate the rate would be $[(49.8 - 43.6)/49.8]$ (100), 12.5%. In this case the rate increase due to external and internal thermal effects more than balances the adverse effect of internal mass-transfer resistance. The procedure for calculating the effects of internal gradients on the rate is presented in Chap. 11.

One additional illustration is of interest. This refers to the hydrofluorination of UO_2 pellets with $\text{HF}(g)$ according to the reaction



This is a different kind of heterogeneous reaction—a gas-solid noncatalytic one. Let us examine the process at initial conditions ($t \rightarrow 0$), so that there has been no opportunity for a layer of $\text{UF}_4(s)$ to be formed around the UO_2 pellet. The process is much like that for gas-solid catalytic reactions. Hydrogen fluoride gas is transferred from the bulk gas to the surface of the UO_2 pellets and reacts at the pellet-gas interface, and H_2O diffuses out into the bulk gas. If the pellet is nonporous, all the reaction occurs at the outer surface of the UO_2 pellet, and only an external transport process is possible. Costa¹ studied this system by suspending spherical pellets 2 cm in diameter in a stirred-tank reactor. In one run, at a bulk-gas temperature of 377°C , the surface temperature was 462°C and the observed rate was $-r_{\text{UO}_2} = 6.9 \times 10^{-6}$ mole $\text{UO}_2/(\text{sec})(\text{cm}^2 \text{ reaction surface})$. At these conditions the concentrations of

¹E. C. Costa and J. M. Smith, *Proc. Fourth European Symp. Chem. Reaction Eng.*, Brussels, September, 1968.

HF gas were 1.12×10^{-5} g mole/cm³ at the surface of the pellet and 1.38×10^{-5} g mole/cm³ in the bulk gas. The intrinsic rate of reaction was found to be given by

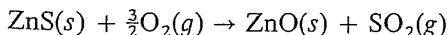
$$r = 40 C_{\text{HF}} e^{-6.070/R_g T} \text{ g mole}/(\text{cm}^2) (\text{sec}) \quad (7-6)$$

where T is in degrees Kelvin and C_{HF} is in gram moles per cubic centimeter. If the rate is evaluated at bulk-gas conditions, Eq. (7-6) gives 5.0×10^{-6} g mole/(sec)(cm²). Then the combined effects of an external temperature and concentration difference serve to increase the rate from 5.0×10^{-6} to 6.9×10^{-6} g mole/(cm²)(sec), or 38%. In this case the temperature at the catalyst surface is 95°C higher than the bulk-gas temperature, and this has a dominating effect on the rate of reaction. The effect of external mass-transfer resistance is to reduce the rate by the ratio of concentrations of HF, 1.12:1.38, or 19%.

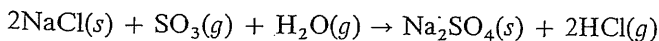
7-2 Types of Heterogeneous Reactions

All the examples in Sec. 7-1 were of the gas-solid form. This is, perhaps, the most important type of heterogeneous system because of its utilization in the chemical industry. Most salable chemicals are prepared by converting raw materials via chemical reactions. Such reactions usually require catalysts, and these are normally solids. Since the temperatures must be high for rapid rates, the reacting fluid commonly is in the gas phase. Examples of large-scale gas-solid catalytic reactions are the major hydrocarbon transformations: cracking, reforming, dehydrogenation (for example, butadiene and butenes from butane), isomerization, desulfurization, etc. Kinetics and reactor design for such systems have naturally received major attention, and most of our emphasis on design is directed to this type (Chap. 13).

Gas-solid heterogeneous reactions may be noncatalytic. An example is the hydrofluorination of uranium dioxide pellets referred to in Sec. 7-1. Since one reactant is in the solid phase and is consumed, the rate of reaction varies with time. Hence such processes are basically transient, in comparison with the steady-state operation of gas-solid catalytic reactors. The process for smelting ores such as zinc sulfide,



is of this type. The conversion of CaCO₃ to CaO in the line kiln is another example. Yet another is the process for making HCl in a transport reactor¹ from salt particles; the reaction is



¹A transport reactor is like a fluidized-bed reactor, except that the fluidized particles move through and out of the reactor with the gas phase.

In many noncatalytic types a solid product builds up around the reacting core [for example, $\text{Na}_2\text{SO}_4(s)$ is deposited around the NaCl particles in the last illustration]. This introduces the additional physical processes of heat and mass transfer through a product layer around the solid reactant. A somewhat different form of noncatalytic gas-solid reaction is the regeneration of catalysts which have been deactivated by the deposition of a substance on the interior surface. The most common is the burning of carbon (with air) which has been gradually deposited on catalyst particles used in hydrocarbon reactions. Many of the physical and chemical steps involved here are the same as those for gas-solid catalytic reactions. The chief difference is the transient nature of the noncatalytic reaction. This type of heterogeneous reaction will be considered in Chap. 14.

Liquid-solid reactions, where the solid phase is a catalyst, is another type of heterogeneous system that is common in the chemical and petroleum industries. Alkylation with $\text{AlCl}_3(s)$ catalyst is an example. In these systems the catalyst frequently forms complexes with reactants and/or products and becomes a poorly defined solid-liquid mixture, best described as a sludge. Analytical treatment in these cases is difficult. An important modification of the liquid-solid catalytic type arises when one reactant is gaseous. Hydrogenation of liquids normally is of this type. A slurry is formed of solid catalyst particles and hydrogen is bubbled into the slurry. These reactions are usually carried out in stirred-tank reactors, where the high heat capacity of the tank contents simplifies temperature control of the exothermic hydrogenation reaction. Such gas-liquid-solid systems involve several physical steps, and indeed, resistance to diffusion of dissolved hydrogen to the catalyst particle is frequently significant. The quantitative treatment of combined physical and chemical steps in such slurry reactors is considered in Chaps. 10 and 13. Polymerization systems are often of this type. For example, ethylene is normally polymerized by dissolving it in a solvent containing suspended catalyst particles. The trickle-bed reactor is a somewhat different form of gas-liquid-solid system. Here gas and liquid, usually in cocurrent flow, pass over a bed of catalyst particles in a fixed bed. This form is used when the volatility of the liquid is so low that complete gasification is not practical. Sulfur compounds are removed from heavy hydrocarbon liquids in such reactors. The gas phase here is primarily hydrogen, which is necessary for the desulfurization reactions.

Liquid-liquid reactions are sometimes encountered. Alkylation of hydrocarbons with aqueous solution of sulfuric acid as a catalyst is an example. As in liquid-solid systems, definition of the liquid phase containing the catalyst may be difficult, reducing the effectiveness of a fundamental analysis in terms of chemical and physical steps.

Solid-solid noncatalytic reactions are important in ceramics manufacture.¹ It appears that diffusion resistances may be important to some extent in all such systems. The diffusion process itself is hard to define in solid-solid systems, since at least two possibilities exist: volume diffusion in the solid² and surface diffusion along interfaces and crystal boundaries.² Little is known about the kinetics of solid-solid reactions at the reacting interface because most measurements include diffusion effects.

Problems

- 7-1. In a sketch similar to Fig. 7-1 show schematically the concentration profiles for a first-order *reversible* catalytic reaction. Consider three cases: (a) reaction control, (b) diffusion control, and (c) an intermediate case.
- 7-2. Explain why mass-transfer resistance reduces the global rate more at higher temperatures than at lower temperatures. Assume no heat-transfer resistance.
- 7-3. For endothermic reactions, do mass- and heat-transfer resistances have complementary or counterbalancing effects on the global rate?
- 7-4. A gaseous reaction with a solid catalyst is carried out in a flow reactor. The system is isothermal, but it is believed that mass-transfer resistances are important. (a) Would increasing the turbulence in the gas region next to the catalyst surface increase or decrease the global rate? (b) If the system is not isothermal and the reaction is exothermic, would increasing the turbulence increase or decrease the global rate?

¹W. Kingery "Kinetics of High Temperature Processes," John Wiley & Sons, Inc., New York, 1959; G. Cohn, *Chem. Rev.*, **42**, 527 (1948).

²R. J. Arrowsmith and J. M. Smith, *Ind. Eng. Chem., Fund. Quart.*, **5**, 327 (1966).

HETEROGENEOUS CATALYSIS

As kinetic information began to accumulate during the last century, it appeared that the rates of a number of reactions were influenced by the presence of a material which itself was unchanged during the process. In 1836 Berzelius¹ reviewed the evidence and concluded that a "catalytic" force was in operation. Among the cases he studied were the conversion of starch into sugar in the presence of acids, the decomposition of hydrogen peroxide in alkaline solutions, and the combination of hydrogen and oxygen on the surface of spongy platinum. In these three examples the acids, the alkaline ions, and the spongy platinum were the materials which increased the rate and yet were virtually unchanged by the reaction. Although the concept of a catalytic force proposed by Berzelius has now been discarded, the term "catalysis" is retained to describe all processes in which the rate of a reaction is influenced by a substance that remains chemically unaffected.

In this chapter we shall consider first the general characteristics of heterogeneous catalysis and adsorption (physical and chemical) and then physical properties of solid catalysts and methods of preparation. Kinetics

¹J. J. Berzelius, *Jahresber. Chem.*, 15, 237 (1836).

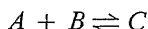
and mechanism of adsorption and fluid-solid catalytic reactions are taken up in Chap. 9.

GENERAL CHARACTERISTICS*

8-1 The Nature of Catalytic Reactions

Although the catalyst remains unchanged at the end of the process, there is no requirement that the material not take part in the reaction. In fact, present theories of catalyst activity postulate that the material does actively participate in the reaction. From the concept of the energy of activation developed in Chap. 2, the mechanism of catalysis would have to be such that the free energy of activation is lowered by the presence of the catalytic material. A catalyst is effective in increasing the rate of a reaction because it makes possible an alternative mechanism, each step of which has a lower free energy of activation than that for the uncatalyzed process. Consider the reaction between hydrogen and oxygen in the presence of spongy platinum. According to the proposed concept, hydrogen combines with the spongy platinum to form an intermediate substance, which then reacts with oxygen to provide the final product and reproduce the catalyst. It is postulated that the steps involving the platinum surface occur at a faster rate than the homogeneous reaction between hydrogen and oxygen.

The combination or complexing of reactant and catalyst is a widely accepted basis for explaining catalysis. For example, suppose the overall reaction



is catalyzed via two active centers, or catalytic sites, X_1 and X_2 , which form complexes with A and B . The reaction is truly catalytic if the sequence of steps is such that the centers X_1 and X_2 are regenerated after they have caused the formation of C . In a general way the process may be written

1. $A + X_1 \rightleftharpoons AX_1$
2. $B + X_2 \rightleftharpoons BX_2$
3. $AX_1 + BX_2 \rightleftharpoons C + X_1 + X_2$

Note that whereas X_1 and X_2 are combined and regenerated a number of times, it does not necessarily follow that their catalyzing ability and/or number remain constant forever. For example, poisons can intervene to slowly remove X_1 and/or X_2 from the system, arresting the catalytic rate. What distinguishes this decline in catalytic activity from that of a non-

*This material was written jointly with Professor J. J. Carberry.

catalytic reaction in which X_1 and X_2 are not regenerated is that the complexing-regenerating sequence occurs a great many times before X_1 and X_2 become inactive. In the noncatalytic sequence no regeneration of X occurs. Hence, while catalysts can deteriorate, their active lifetime is far greater than the time required for reaction.

A relatively small amount of catalyst can cause conversion of a large amount of reactant. For example, Glasstone¹ points out that cupric ions in the concentration of 10^{-9} mole/liter appreciably increase the rate of the oxidation of sodium sulfide by oxygen. However, the idea that a small amount of the catalyst can cause a large amount of reaction does not mean that the catalyst concentration is unimportant. In fact, when the reaction does not entail a chain mechanism, the rate of the reaction is usually proportional to the concentration of the catalyst. This is perhaps most readily understood by considering the case of surface catalytic reactions. In the reaction of hydrogen and oxygen with platinum catalyst the rate is found to be directly proportional to the platinum surface. Here a simple proportionality exists between platinum surface area and the number of centers X which catalyze the oxidation of hydrogen. While a simple relationship may not often exist in solid-catalyzed reactions, in homogeneous catalysis there is often a direct proportionality between rate and catalyst concentration. For example, the hydrolysis of esters in an acid solution will depend on the concentration of hydrogen ion acting as a catalyst.

The position of equilibrium in a reversible reaction is not changed by the presence of the catalyst. This conclusion has been verified experimentally in several instances. For example, the oxidation of sulfur dioxide by oxygen has been studied with three catalysts: platinum, ferric oxide, and vanadium pentoxide. In all three cases the *equilibrium compositions* were the same.

An important characteristic of a catalyst is its effect on selectivity when several reactions are possible. A good illustration is the decomposition of ethanol. Thermal decomposition gives water, acetaldehyde, ethylene, and hydrogen. If, however, ethanol vapor is suitably contacted with alumina particles, ethylene and water are the only products. In contrast, dehydrogenation to acetaldehyde is virtually the sole reaction when ethanol is reacted over a copper catalyst.

The general characteristics of catalysis may be summarized as follows:

1. A catalyst accelerates reaction by providing alternate paths to products, the activation energy of each catalytic step being less than that for the homogeneous (noncatalytic) reaction.
2. In the reaction cycle active centers of catalysis are combined with at

¹S. Glasstone, "Textbook of Physical Chemistry," p. 1104, D. Van Nostrand Company, Inc., New York, 1940.

least one reactant and then freed with the appearance of product. The freed center then recombines with reactant to produce another cycle, and so on.

3. Comparatively small quantities of catalytic centers are required to produce large amounts of product.
4. Equilibrium conversion is not altered by catalysis. A catalyst which accelerates the forward reaction in an equilibrium system is a catalyst for the reverse reaction.
5. The catalyst can radically alter selectivity.

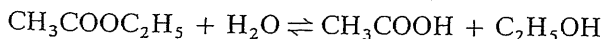
Examples have been observed of negative catalysis, where the rate is decreased by the catalyst. Perhaps the most reasonable theory is that developed for chain reactions. In these cases it is postulated that the catalyst breaks the reaction chains, or sequence of steps, in the mechanism. For example, nitric oxide reduces the rate of decomposition of acetaldehyde and ethyl ether. Apparently nitric oxide has the characteristic of combining with the free radicals involved in the reaction mechanism. The halogens, particularly iodine, also act as negative catalysts in certain gaseous reactions. In the combination of hydrogen and oxygen, where a chain mechanism is probably involved, iodine presumably destroys the radicals necessary for the propagation of the chains.

8-2 *The Mechanism of Catalytic Reactions*

The concept that a catalyst provides an alternate mechanism for accomplishing a reaction, and that this alternate path is a more rapid one, has been developed in many individual cases. The basis of this idea is that the catalyst and one or more of the reactants form an intermediate complex, a loosely bound compound which is unstable, and that this complex then takes part in subsequent reactions which result in the final products and the regenerated catalyst. Homogeneous catalysis can frequently be explained in terms of this concept. For example, consider catalysis by acids and bases. In aqueous solutions acids and bases can increase the rate of hydrolysis of sugars, starches, and esters. The kinetics of the hydrolysis of ethyl acetate catalyzed by hydrochloric acid can be explained by the following mechanism:

1. $\text{CH}_3\text{COOC}_2\text{H}_5 + \text{H}^+ \rightleftharpoons \text{CH}_3\text{COOC}_2\text{H}_5[\text{H}^+]$
2. $\text{CH}_3\text{COOC}_2\text{H}_5[\text{H}^+] + \text{H}_2\text{O} \rightleftharpoons \text{C}_2\text{H}_5\text{OH} + \text{H}^+ + \text{CH}_3\text{COOH}$

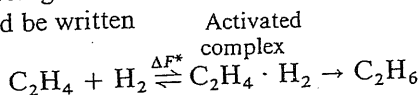
For this catalytic sequence to be rapid with respect to noncatalytic hydrolysis, the free energy of activation of reaction steps 1 and 2 must each be less than the free energy of activation for the noncatalytic reaction,



Similarly, the heterogeneous catalytic hydrogenation of ethylene on a solid catalyst might be represented by the steps

1. $C_2H_4 + X_1 \xrightleftharpoons{\Delta F_1} C_2H_4X_1$
2. $H_2 + X_1C_2H_4 \xrightleftharpoons{\Delta F_2} C_2H_4[X_1]H_2$
3. $C_2H_4[X_1]H_2 \xrightleftharpoons{\Delta F_3} C_2H_6 + X_1$

where $[X_1]$ is the solid catalyst and $C_2H_4[X_1]H_2$ represents the complex formed between the reactants and the catalyst. The homogeneous reaction, according to the absolute theory of reaction rates discussed in Chap. 2, would be written



where the free-energy change for the formation of the activated complex ΔF^* is the free energy of activation for the homogeneous reaction. The effectiveness of the catalyst is explained on the basis that the free energy of activation of each of the steps in the catalytic mechanism is less than ΔF^* .

These illustrations, particularly that for ethylene hydrogenation, are grossly oversimplified. They must be considered phenomenological models, not mechanisms. The actual mechanism of ethylene hydrogenation is quite complex. In spite of the considerable effort focused on this reaction, a mechanism satisfactory to all investigators has yet to be offered. The system does, however, provide an opportunity to compare homogeneous and heterogeneous rates. Using published data, Boudart¹ found that the homogeneous and catalytic rates can be expressed as

$$\begin{aligned} r_{\text{hom}} &= 10^{27} e^{-43,000/R_g T} \\ r_{\text{cat}} &= 2 \times 10^{27} e^{-13,000/R_g T} \quad (\text{CuO-MgO catalyst}) \end{aligned}$$

At 600°K the relative rates are

$$\frac{r_{\text{cat}}}{r_{\text{hom}}} = e^{(43,000-13,000)/600 R_g} \simeq 10^{11}$$

In this case the catalyst has caused a radical reduction in overall activation energy, presumably by replacing a difficult homogeneous step by a more easily executed surface reaction involving adsorbed ethylene. The results lead to the kinetics observed by Wynkoop and Wilhelm,² a reaction first order in H_2 and zero order in strongly adsorbed ethylene.

¹ M. Boudart, *Ind. Chim. Belg.*, 23, 383 (1958).

² R. Wynkoop and R. H. Wilhelm, *Chem. Eng. Progr.*, 46, 300 (1950).

The three steps postulated for the catalytic hydrogenation of ethylene indicate that the rate may be influenced by both adsorption and desorption (steps 1 and 3) and the surface reaction (step 2). Two extreme cases can be imagined: that step 1 or step 3 is slow with respect to step 2 or that step 2 is relatively slow. In the first situation rates of adsorption or desorption are of interest, while in the second the surface concentration of the adsorbed species corresponding to equilibrium with respect to steps 1 and 3 is needed. In any case we should like to know the number of sites on the catalyst surface, or at least the surface area of the catalyst. These questions require a study of adsorption. More is known about adsorption of gases, and this will be emphasized in the sections that follow.

ADSORPTION ON SOLID SURFACES

8-3 Surface Chemistry and Adsorption

Even the most carefully polished surfaces are not smooth in a microscopic sense, but are irregular, with valleys and peaks alternating over the area. The regions of irregularity are particularly susceptible to residual force fields. At these locations the surface atoms of the solid may attract other atoms or molecules in the surrounding gas or liquid phase. Similarly, the surfaces of pure crystals have nonuniform force fields because of the atomic structure in the crystal. Such surfaces also have sites or active centers where adsorption is enhanced. Two types of adsorption may occur.

Physical Adsorption¹ The first type of adsorption is nonspecific and somewhat similar to the process of condensation. The forces attracting the fluid molecules to the solid surface are relatively weak, and the heat evolved during the adsorption process is of the same order of magnitude as the heat of condensation, 0.5 to 5 kcal/g mole. Equilibrium between the solid surface and the gas molecules is usually rapidly attained and easily reversible, because the energy requirements are small. The energy of activation for physical adsorption is usually no more than 1 kcal/g mole. This is a direct consequence of the fact that the forces involved in physical adsorption are weak. Physical adsorption cannot explain the catalytic activity of solids for reactions between relatively stable molecules, because there is no possibility of large reductions in activation energy. Reactions of atoms and free radicals at surfaces sometimes involve small activation energies, and in these cases physical adsorption may play a

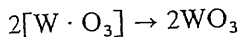
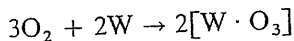
¹For a detailed treatment of physical adsorption see D. M. Young and A. D. Crowell, "Physical Adsorption of Gases," Butterworths & Co. (Publishers), London, 1962.

role. Also, physical adsorption serves to concentrate the molecules of a substance at a surface. This can be of importance in cases involving reaction between a chemisorbed reactant and a coreactant which can be physically adsorbed. In such a system the catalytic reaction would occur between chemisorbed and physically adsorbed reactants. Catalysis cannot be attributed solely to physical adsorption. Thus *all* solids will physically adsorb gases under suitable conditions, and yet all solids are not catalysts.

The amount of physical adsorption decreases rapidly as the temperature is raised and is generally very small above the critical temperatures of the adsorbed component. This is further evidence that physical adsorption is not responsible for catalysis. For example, the rate of oxidation of sulfur dioxide on a platinum catalyst becomes appreciable only above 300°C; yet this is considerably above the critical temperature of sulfur dioxide (157°C) or of oxygen (-119°C). Physical adsorption is not highly dependent on the irregularities in the nature of the surface, but is usually directly proportional to the amount of surface. However, the extent of adsorption is not limited to a monomolecular layer on the solid surface, especially near the condensation temperature. As the layers of molecules build up on the solid surface, the process becomes progressively more like one of condensation.

Physical-adsorption studies are valuable in determining the physical properties of solid catalysts. Thus the questions of surface area and pore-size distribution in porous catalysts can be answered from physical-adsorption measurements. These aspects of physical adsorption are considered in Secs. 8-5 and 8-7.

Chemisorption¹ The second type of adsorption is specific and involves forces much stronger than in physical adsorption. According to Langmuir's pioneer work,² the adsorbed molecules are held to the surface by valence forces of the same type as those occurring between atoms in molecules. He observed that a stable oxide film was formed on the surface of tungsten wires in the presence of oxygen. This material was not the normal oxide WO₃, because it exhibited different chemical properties. However, analysis of the walls of the vessel holding the wire indicated that WO₃ was given off from the surface upon desorption. This suggested a process of the type



¹For a detailed treatment of chemisorption see D. O. Hayward and B. M. W. Trapnell, "Chemisorption," 2d ed., Butterworths & Co. (Publishers), London, 1964.

²I. Langmuir, *J. Am. Chem. Soc.*, 38, 221 (1916).

where $[W \cdot O_3]$ represents the adsorbed compound. Further evidence for the theory that such adsorption involves valence bonds is found in the large heats of adsorption. Observed values are of the same magnitude as the heat of chemical reactions, 5 to 100 kcal/g mole.

Taylor¹ suggested the name *chemisorption* for describing this second type of combination of gas molecules with solid surfaces. Because of the high heat of adsorption, the energy possessed by chemisorbed molecules can be substantially different from that of the molecules alone. Hence the energy of activation for reactions involving chemisorbed molecules can be considerably less than that for reactions involving the molecules alone. It is on this basis that chemisorption offers an explanation for the catalytic effect of solid surfaces.

Two kinds of chemisorption are encountered: activated and, less frequently, nonactivated. *Activated chemisorption* means that the rate varies with temperature according to a finite activation energy in the Arrhenius equation. However, in some systems chemisorption occurs very rapidly, suggesting an activation energy near zero. This is termed *nonactivated chemisorption*.² It is often found that for a given gas and solid the initial chemisorption is nonactivated, while later stages of the process are slow and temperature dependent (activated adsorption).

With respect to adsorption *equilibrium*, the relationship between temperature and quantity adsorbed (both physically and chemically) is shown in Fig. 8-1. Chemisorption is assumed to be activated in this case.

As the critical temperature of the component is exceeded, physical adsorption approaches a very low equilibrium value. As the temperature is raised, the amount of activated adsorption becomes important because the rate is high enough for significant quantities to be adsorbed in a reasonable amount of time. In an ordinary adsorption experiment involving the usual time periods the adsorption curve actually rises with increasing temperatures from the minimum value, as shown by the solid line in Fig. 8-1. When the temperature is increased still further, the decreasing equilibrium value for activated adsorption retards the process, and the quantity adsorbed passes through a maximum. At these high temperatures even the rate of the relatively slow activated process may be sufficient to give results closely approaching equilibrium. Hence the solid curve representing the amount adsorbed approaches the dashed equilibrium value for the activated adsorption process.

It has been explained that the effectiveness of solid catalysts for reactions of stable molecules is dependent upon chemisorption. Granting

¹H. S. Taylor, *J. Am. Chem. Soc.*, 53, 578 (1931).

²As an illustration, chemisorption of hydrogen on nickel at low temperatures is nonactivated; see G. Padberg and J. M. Smith, *J. Catalysis*, 12, 111 (1968).

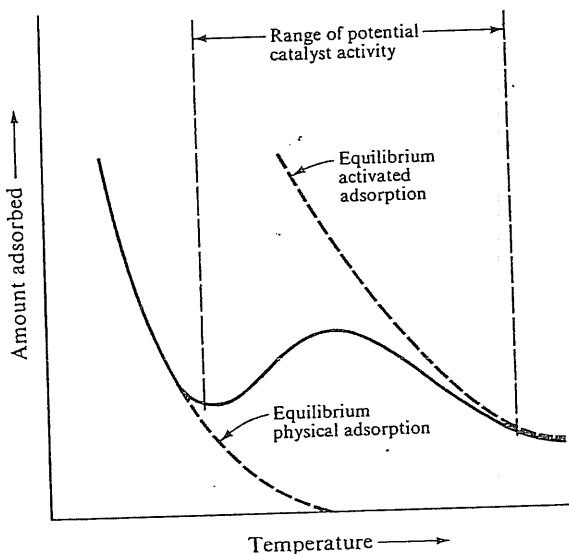


Fig. 8-1 Effect of temperature on physical and activated adsorption.

this, the temperature range over which a given catalyst is effective must coincide with the range where chemisorption of one or more of the reactants is appreciable. This is indicated on Fig. 8-1 by the dashed vertical lines. There is a relationship between the extent of chemisorption of a gas on a solid and the effectiveness of the solid as a catalyst. For example, many metallic and metal-oxide surfaces adsorb oxygen easily, and these materials are also found to be good catalysts for oxidation reactions. When reactions proceed catalytically at low temperatures, Fig. 8-1 does not apply. In these cases catalysis is due to nonactivated chemisorption. Thus ethylene is hydrogenated on nickel at -78°C , at which temperature there would surely exist physical adsorption of the ethylene.

An important feature of chemisorption is that its magnitude will not exceed that corresponding to a monomolecular layer. This limitation is due to the fact that the valence forces holding the molecules on the surface diminish rapidly with distance. These forces become too small to form the adsorption compound when the distance from the surface is much greater than the usual bond distances.

The differences between chemisorption and physical adsorption are summarized in Table 8-1.

The key concept for quantitative treatment of both physical and chemical adsorption is that formulated by Langmuir.¹ While his concern

¹I. Langmuir, *J. Am. Chem. Soc.*, 40, 1361 (1918).

Table 8-1 Physical vs chemical adsorption

Parameter	Physical adsorption	Chemisorption
Adsorbent, Adsorbate	All solids All gases below critical temperature	Some solids Some chemically reactive gases
Temperature range	Low temperature	Generally high temperature
Heat of adsorption	Low ($\approx \Delta H_{\text{cond}}$)	High, order of heat of reaction
Rate (activation energy)	Very rapid, low E	Nonactivated, low E ; activated, high E
Coverage	Multilayer possible	Monolayer
Reversibility	Highly reversible	Often irreversible
Importance	For determination of surface area and pore size	For determination of active-center area and elucidation of surface- reaction kinetics

was with chemisorption, Brunauer, Emmett, and Teller gainfully employed the concepts to derive a valuable relationship between the volume of a gas physically adsorbed and total surface area of the adsorbent (see Sec. 8-5). Also, the Langmuir treatment can be extended to develop useful relations for chemisorption rates and rate of catalytic reactions, even for surfaces which do not obey the basic postulates of the Langmuir theory. This second application is given in Chap. 9.

8-4 The Langmuir Treatment of Adsorption

The derivations may be carried out by using as a measure of the amount adsorbed either the fraction of the surface covered or the concentration of the gas adsorbed on the surface. Both procedures will be illustrated, although the second is the more useful for kinetic developments (Chap. 9). The important assumptions are as follows:¹

1. All the surface of the catalyst has the same activity for adsorption; i.e., it is energetically uniform. The concept of nonuniform surface with active centers can be employed if it is assumed that all the active centers have the same activity for adsorption and that the rest of the surface has none, or that an average activity can be used.
2. There is no interaction between adsorbed molecules. This means that the amount adsorbed has no effect on the rate of adsorption per site.

¹It is also tacitly supposed that each site can accommodate only one adsorbed particle.

3. All the adsorption occurs by the same mechanism, and each adsorbed complex has the same structure.
4. The extent of adsorption is less than one complete monomolecular layer on the surface.

In the system of solid surface and gas, the molecules of gas will be continually striking the surface and a fraction of these will adhere. However, because of their kinetic, rotational, and vibrational energy, the more energetic molecules will be continually leaving the surface. An equilibrium will be established such that the rate at which molecules strike the surface, and remain for an appreciable length of time, will be exactly balanced by the rate at which molecules leave the surface.

The rate of adsorption r_a will be equal to the rate of collision r_c of molecules with the surface multiplied by a factor F representing the fraction of the colliding molecules that adhere. At a fixed temperature the number of collisions will be proportional to the pressure p of the gas, and the fraction F will be constant. Hence the rate of adsorption per unit of bare surface will be $r_c F$. This is equal to kp , where k is a constant involving the fraction F and the proportionality between r_c and p .

Since the adsorption is limited to complete coverage by a monomolecular layer, the surface may be divided into two parts: the fraction θ covered by the adsorbed molecules and the fraction $1 - \theta$, which is bare. Since only those molecules striking the uncovered part of the surface can be adsorbed, the rate of adsorption per unit of total surface will be proportional to $1 - \theta$; that is,

$$r_a = kp(1 - \theta) \quad (8-1)$$

The rate of desorption will be proportional to the fraction of covered surface

$$r_d = k'\theta \quad (8-2)$$

The amount adsorbed at equilibrium is obtained by equating r_a and r_d and solving for θ . The result, called the *Langmuir isotherm*, is

$$\theta = \frac{kp}{k' + kp} = \frac{Kp}{1 + Kp} = \frac{v}{v_m} \quad (8-3)$$

where $K = k/k'$ is the adsorption equilibrium constant, expressed in units of $(\text{pressure})^{-1}$. The fraction θ is proportional to volume of gas adsorbed, v , since the adsorption is less than a monomolecular layer. Hence Eq. (8-3) may be regarded as a relationship between the pressure of the gas and the volume adsorbed. This is indicated by writing $\theta = v/v_m$, where v_m is the volume adsorbed when all the active sites are covered, i.e., when there is a complete monomolecular layer.

The concentration form of Eq. (8-3) can be obtained by introducing the concept of an adsorbed concentration \bar{C} , expressed in moles per gram of catalyst. If \bar{C}_m represents the concentration corresponding to a complete monomolecular layer on the catalyst, then the rate of adsorption, moles/(sec) (g catalyst) is, by analogy with Eq. (8-1),

$$r_a = k_c C_g (\bar{C}_m - \bar{C}) \quad (8-4)$$

where k_c is the rate constant for the catalyst and C_g is the concentration of adsorbable component in the gas. Similarly, Eq. (8-2) becomes

$$r_d = k'_c \bar{C} \quad (8-5)$$

At equilibrium the rates given by Eqs. (8-4) and (8-5) are equal, so that

$$\bar{C} = \frac{K_c \bar{C}_m C_g}{1 + K_c C_g} \quad (8-6)$$

where now the equilibrium constant K_c is equal to k_c/k'_c and is expressed in cubic centimeters per gram mole. Since $\bar{C}/\bar{C}_m = \theta$, Eq. (8-6) may also be written

$$\theta = \frac{K_c C_g}{1 + K_c C_g} \quad (8-7)$$

which is a form analogous to Eq. (8-3), since C_g is proportional to p .

Equation (8-6) predicts that adsorption data should have the general form shown in Fig. 8-2. Note that at low values of C_g (or low surface coverages θ) the expression becomes a straight line with a slope equal to $K_c \bar{C}_m$. The data points in Fig. 8-2 are for the physical adsorption of *n*-butane on silica gel ($S_g = 832 \text{ m}^2/\text{g}$) at 50°C .¹ The solid line represents Eq. (8-6), where

$$\bar{C}_m = 0.85 \times 10^{-3} \text{ g mole/g silica gel}$$

and the equilibrium constant of adsorption is

$$K_c = 4.1 \times 10^5 \text{ cm}^3/\text{g mole}$$

For this instance of physical adsorption Eq. (8-6) fits the data rather well. The measurements were made on mixtures of *n*-butane in helium (at 1 atm total pressure) to vary C_g . The percentage of *n*-butane in the gas corresponding to the concentration C_g is shown as a second abscissa in the figure. Also, θ is shown as a second ordinate. This was calculated from $\theta = \bar{C}/\bar{C}_m$. It is interesting to note that the isotherm is linear up to about $\theta = 0.10$, or 10% surface coverage.

¹Data from R. L. Cerro, "Adsorption Studies by Chromatography," master's thesis, University of California, Davis, Calif., September, 1968.

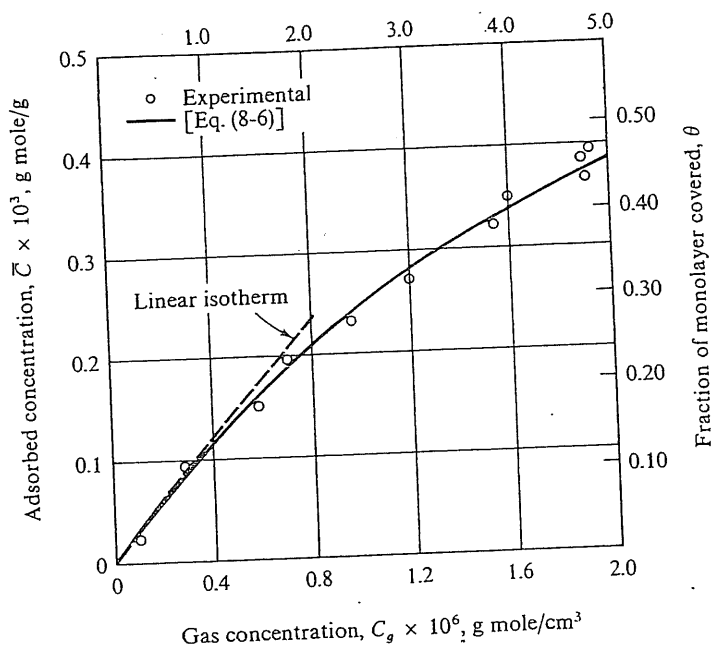


Fig. 8-2 Adsorption-equilibrium data for *n*-butane on silica gel (surface area 832 m²/g) at 50°C

Chemisorption data often do not fit Eq. (8-6). However, the basic concepts on which the Langmuir isotherm is based, the ideas of a dynamic equilibrium between rates of adsorption and desorption and a finite adsorption time, are sound and of great value in developing the kinetics of fluid-solid catalytic reactions. Equations (8-4) to (8-6) form the basis for the rate equations presented in Chap. 9.

PHYSICAL PROPERTIES OF CATALYSTS

The surface area of a solid has a pronounced effect on the amount of gas adsorbed and on its activity as a catalyst. For example, if a sample of fresh Raney nickel, which is highly porous and has a large surface, is held in the hand, the heat due to adsorption of oxygen can be felt immediately. No heat is apparent in the same mass of nonporous nickel. This relationship between surface area and extent of adsorption has led to the development of highly porous materials with areas as high as 1,500 m²/g. Sometimes the catalytic material itself can be prepared in a form with large surface area. When this is not possible, materials which can be so prepared may

be used as a carrier or support on which the catalytic substance is dispersed. Silica gel and alumina are widely used as supports.

The dependence of rates of adsorption and catalytic reactions on surface makes it imperative to have a reliable method of measuring surface area. Otherwise it would not be possible to compare different catalysts (whose areas are different) to ascertain the intrinsic activity per unit surface. For surface areas in the range of hundreds of square meters per gram a porous material with equivalent cylindrical pore radii (see Sec. 8-5) in the range of 10 to 100 Å is needed. The following example shows that such areas are not possible with nonporous particles of the size which can be economically manufactured.

Example 8-1 Spray drying and other procedures for manufacturing small particles can produce particles as small as 2 to 5 microns. Calculate the external surface area of nonporous spherical particles of 2 microns diameter. What size particles would be necessary if the external surface is to be 100 m²/g? The density of the particles is 2.0 g/cm³.

Solution The external surface area per unit volume of a spherical particle of diameter d_p is

$$\frac{\pi d_p^2}{\pi d_p^3/6} = \frac{6}{d_p}$$

If the particle density is ρ_p , the surface area, per gram of particles, would be

$$S_g = \frac{6}{\rho_p d_p}$$

For $d_p = 2$ microns (2×10^{-4} cm) and $\rho_p = 2.0$ g/cm³

$$S_g = \frac{6}{2(2 \times 10^{-4})} = 1.5 \times 10^4 \text{ cm}^2/\text{g}$$

or

$$S_g = 1.5 \text{ m}^2/\text{g}$$

This is about the largest surface area to be expected for nonporous particles. If a surface of 100 m²/g were required, the spherical particles would have a diameter of

$$d_p = \frac{6}{\rho_p S_g} = \frac{6}{2.0(100 \times 10^4)} = 0.02 \times 10^{-4} \text{ cm}$$

or

$$d_p = 0.02 \text{ micron}$$

Particles as small as this cannot, at present, be produced on a commercial scale. It may be noted that the smaller particles found in a fluidized-bed reactor are retained on 400 mesh size, which has a sieve opening of 37 microns.

When the major catalytic surface is in the interior of a solid particle, the resistance to transport of mass and energy from the external surface to the interior can have a significant effect on the global rate of reaction. Quantitative treatment of this problem is the objective in Chap. 11. It is sufficient here to note that this treatment rests on a geometric model for the extent and distribution of void spaces within the complex porous structure of the particle. It would be best to know the size and shape of each void space in the particle. In the absence of this information the parameters in the model should be evaluated from reliable and readily obtainable geometric properties. In addition to the surface area, three other properties fall into this classification: void volume, the density of the solid material in the particle, and the distribution of void volume according to void size (pore-volume distribution). The methods of measurement of these four properties are considered in Secs. 8-5 to 8-7.

8-5 Determination of Surface Area

The standard method for measuring catalyst areas is based on the physical adsorption of a gas on the solid surface. Usually the amount of nitrogen adsorbed at equilibrium at the normal boiling point (-195.8°C) is measured over a range of nitrogen pressures below 1 atm. Under these conditions several layers of molecules may be adsorbed on top of each other on the surface. The amount adsorbed when one molecular layer is attained must be identified in order to determine the area. The historical steps in the development of the Brunauer-Emmett-Teller method¹ are clearly explained by Emmett.² There may be some uncertainty as to whether the values given by this method correspond exactly to the surface area. However, this is relatively unimportant, since the procedure is standardized and the results are reproducible. It should be noted that the surface area so measured may not be the area effective for catalysis. For example, only certain parts of the surface, the active centers, may be active for chemisorption, while nitrogen may be physically adsorbed on much more of the surface. Also, when the catalyst is dispersed on a large-area support, only part of the support area may be covered by catalytically active atoms. For example, a nickel-on-kieselguhr catalyst was found to have a surface of $205\text{ m}^2/\text{g}$ as measured by nitrogen adsorption.³ To determine the area covered by nickel atoms, hydrogen was chemisorbed on the catalyst at 25°C . From the amount of hydrogen chemisorbed, the surface area of nickel atoms was calculated to be about $40\text{ m}^2/\text{g}$. It would be most useful to know surface areas for

¹S. Brunauer, P. H. Emmett, and E. Teller, *J. Am. Chem. Soc.*, **60**, 309 (1938).

²P. H. Emmett (ed.), "Catalysis," vol. I, chap. 2, Reinhold Publishing Corporation, New York, 1954.

³G. Padberg and J. M. Smith, *J. Catalysis*, **12**, 111 (1968).

chemisorption of the reactant at reaction conditions. However, this would require measurement of relatively small amounts of chemisorption at different, and often troublesome, conditions (high temperature and/or pressure), for each reaction system. In contrast, nitrogen can be adsorbed easily and rapidly in a routine fashion with standard equipment.

In the classical method of determining surface area an all-glass apparatus is used to measure the volume of gas adsorbed on a sample of the solid material.¹ The apparatus operates at a low pressure which can be varied from near zero up to about 1 atm. The operating temperature is in the range of the normal boiling point. The data obtained are gas volumes at a series of pressures in the adsorption chamber. The observed volumes are normally corrected to cubic centimeters at 0°C and 1 atm (standard temperature and pressure) and plotted against the pressure in millimeters, or as the ratio of the pressure to the vapor pressure at the operating temperature. Typical results from Brunauer and Emmett's work² are shown in Fig. 8-3 for the adsorption of several gases on a 0.606-g sample of silica gel. To simplify the classical experimental procedure a flow method has been developed in which a mixture of helium and the gas to be adsorbed is passed continuously over the sample of solid.³ The operating total pressure is constant, and the partial pressure of adsorbable gas is varied by changing the composition of the mixture. The procedure⁴ is to pass a mixture of known composition over the sample until equilibrium is reached, that is, until the solid has adsorbed an amount of adsorbable component corresponding to equilibrium at its partial pressure in the mixture. Then the gas is desorbed by heating the sample while a stream of pure helium flows over it. The amount desorbed is measured with a thermal-conductivity cell or other detector. This gives one point on an isotherm, such as shown in Fig. 8-3. Then the process is repeated at successively different compositions of the mixture until the whole isotherm is obtained.

The curves in Fig. 8-3 are similar to the extent that at low pressures they rise more or less steeply and then flatten out for a linear section at intermediate pressures. After careful analysis of much data it was concluded that the lower part of the linear region corresponded to complete monomolecular adsorption. If this point could be located with precision, the

¹For a complete description of apparatus and techniques see L. G. Joyner, "Scientific and Industrial Glass Blowing and Laboratory Techniques," Instruments Publishing Company, Pittsburgh, 1949; see also S. Brunauer, "The Adsorption of Gases and Vapors," vol. 1, Princeton University Press, Princeton, N.J., 1943.

²S. Brunauer and P. H. Emmett, *J. Am. Chem. Soc.*, **59**, 2682 (1937).

³F. M. Nelson and F. T. Eggertsen, *Anal. Chem.*, **30**, 1387 (1958).

⁴A description of the operating procedure and the data obtained are given by S. Masamune and J. M. Smith [*AIChE J.*, **10**, 246 (1964)] for the adsorption of nitrogen on Vycor (porous glass).

volume of one monomolecular layer of gas, v_m , could then be read from the curve and the surface area evaluated. The Brunauer-Emmett-Teller method locates this point from an equation obtained by extending the Langmuir isotherm to apply to multilayer adsorption. The development is briefly summarized as follows: Equation (8-3) can be rearranged to the form

$$\frac{p}{v} = \frac{1}{Kv_m} + \frac{p}{v_m} \quad (8-8)$$

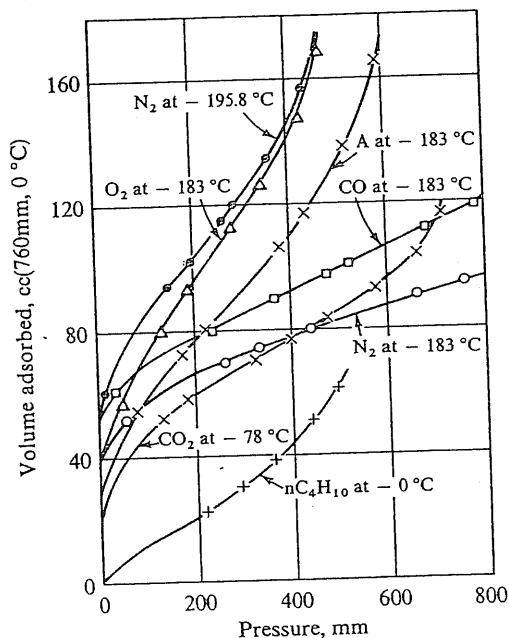
Brunauer, Emmett, and Teller adapted this equation for multilayer adsorption and arrived at the result

$$\frac{p}{v(p_0 - p)} = \frac{1}{v_m c} + \frac{(c - 1)p}{cv_m p_0} \quad (8-9)$$

where p_0 is the saturation or vapor pressure and c is a constant for the particular temperature and gas-solid system.

According to Eq. (8-9), a plot of $p/v(p_0 - p)$ vs p/p_0 should give a straight line. The data of Fig. 8-3 are replotted in this fashion in Fig. 8-4.

Fig. 8-3 Adsorption isotherms for various gases on a 0.606-g sample of silica gel [by permission from P. H. Emmett (ed.), "Catalysis," vol. I, Reinhold Publishing Corporation, New York, 1954]



Of additional significance is the fact that such straight lines can be safely extrapolated to $p/p_0 = 0$. The intercept I obtained from this extrapolation, along with the slope s of the straight line, gives two equations from which v_m can be obtained,

$$I = \frac{1}{v_m c} \quad \text{at } p/p_0 = 0 \quad (8-10)$$

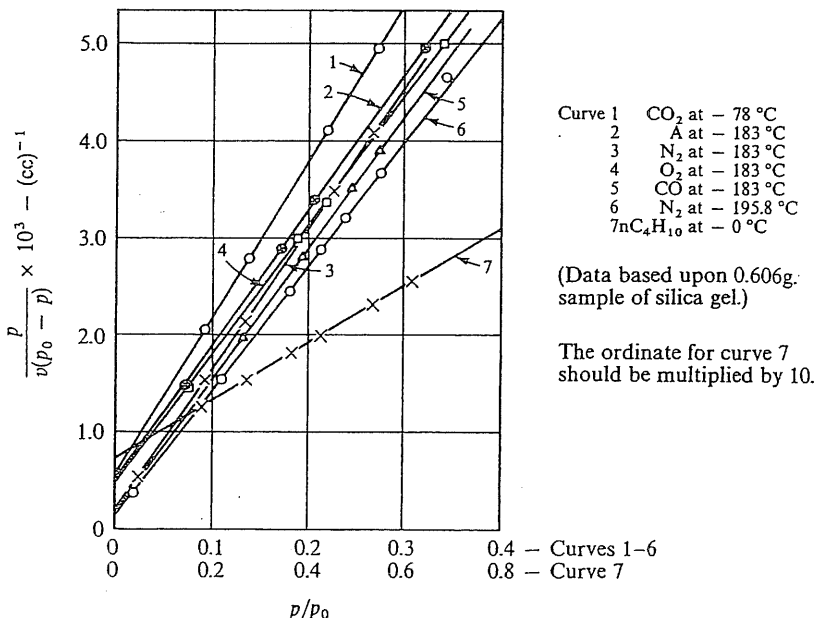
$$s = \frac{c - 1}{v_m c} \quad (8-11)$$

Solving these equations for the volume of adsorbed gas corresponding to a monomolecular layer gives

$$v_m = \frac{1}{I + s} \quad (8-12)$$

The volume v_m can be readily converted to the number of molecules adsorbed. However, to determine the absolute surface area it is necessary to select a value for the area covered by one adsorbed molecule. If this is α , the total surface area is given by

Fig. 8-4 Plot of Brunauer-Emmett-Teller equation [Eq. (8-9)] for data of Fig. 8-3 [by permission from P. H. Emmett (ed.), "Catalysis," vol. 1, Reinhold Publishing Corporation, New York, 1954]



$$S_g = \left[\frac{v_m N_0}{V} \right] \alpha \quad (8-13)$$

where N_0 is Avogadro's number, 6.02×10^{23} molecules/mole, and V is the volume per mole of gas at conditions of v_m . Since v_m is recorded at standard temperature and pressure, $V = 22,400 \text{ cm}^3/\text{g mole}$. The term in brackets represents the number of molecules adsorbed. If v_m is based on a 1.0 g sample, then S_g is the total surface per gram of solid adsorbent.

The value of α has been the subject of considerable investigation. Emmett and Brunauer¹ proposed that α is the projected area of a molecule on the surface when the molecules are arranged in close two-dimensional packing. This value is slightly larger than that obtained by assuming that the adsorbed molecules are spherical and their projected area on the surface is circular. The proposed equation is

$$\alpha = 1.09 \left[\frac{M}{N_0 \rho} \right]^{2/3} \quad (8-14)$$

where M is molecular weight and ρ is the density of the adsorbed molecules. The term in brackets represents the volume of one adsorbed molecule. The density is normally taken as that of the pure liquid at the temperature of the adsorption experiment. For example, for N_2 at -195.8°C , $\rho = 0.808 \text{ g/cm}^3$.

In theory, the adsorption measurements can be made with a number of different gases. However, it has been found that even when values of α are calculated from Eq. (8-14) for each gas the results are somewhat different (see Example 8-3). Therefore it has become standard procedure to employ N_2 at its normal boiling point (-195.8°C). The reason for the variation in areas obtained with different gases is not well understood. Nevertheless, if the measurements are carried out with one gas at one temperature, the results for different catalysts may be compared with confidence.

With the value of ρ for N_2 at -195.8°C , the area per molecule from Eq. (8-14) is $16.2 \times 10^{-16} \text{ cm}^2$, or 16.2 \AA^2 . If this result is used in Eq. (8-13), along with the known values of N_0 and V , the surface area per gram is

$$S_g = 4.35 \times 10^4 v_m \quad \text{cm}^2/\text{g solid adsorbent} \quad (8-15)$$

Remember in using Eq. (8-15) that it is based on adsorption measurements with N_2 at -195.8°C .

Table 8-2 shows surface areas determined by the Brunauer-Emmett-

¹P. H. Emmett and S. Brunauer, *J. Am. Chem. Soc.*, 59, 1553 (1937).

Table 8-2 Surface area, pore volume, and mean pore radii for typical solid catalysts

Catalyst	Surface area, m ² /g	Pore volume, cm ³ /g	Mean pore radius, Å
Activated carbons	500-1,500	0.6-0.8	10-20
Silica gels	200-600	0.4	15-100
SiO-Al ₂ O ₃ cracking catalysts	200-500	0.2-0.7	33-150
Activated clays	150-225	0.4-0.52	100
Activated alumina	175	0.39	45
Celite (Kieselguhr)	4.2	1.1	11,000
Synthetic ammonia catalysts, Fe	...	0.12	200-1,000
Pumice	0.38		
Fused copper	0.23		

SOURCE: In part from A. Wheeler, "Advances in Catalysis," vol. III, pp. 250-326, Academic Press, Inc., New York, 1950.

Teller method for a number of common catalysts and carriers. Calculations of surface areas from adsorption data are illustrated in Examples 8-2 and 8-3.

Example 8-2 From the Brunauer-Emmett-Teller plot in Fig. 8-4 estimate the surface area per gram of the silica gel. Use the data for adsorption of nitrogen at -195.8°C .

Solution From curve 6 of Fig. 8-4, the intercept on the ordinate is

$$I = 0.1 \times 10^{-3} \text{ cm}^{-3}$$

The slope of the curve is

$$s = \frac{(5.3 - 0.1) \times 10^{-3}}{0.4 - 0} = 13 \times 10^{-3} \text{ cm}^{-3}$$

These values of s and I may be substituted in Eq. (8-12) to obtain v_m ,

$$v_m = \frac{10^3}{0.1 + 13} \frac{1}{0.606} = 126 \text{ cm}^3/\text{g catalyst}$$

The factor 0.606 is introduced because the data in Fig. 8-4 are for a silica gel sample of 0.606 g, and v_m is the monomolecular volume per gram. For nitrogen at -195.8°C , the application of Eq. (8-15) yields

$$S_g = 4.35(126) = 550 \text{ m}^2/\text{g}$$

Example 8-3 For comparison, estimate the surface area of the silica gel by using the adsorption data for oxygen at -183°C . The density of the liquefied oxygen at -183°C , from the International Critical Tables, is 1.14 g/cm.

Solution First the area of an adsorbed molecule of O_2 must be calculated from Eq. (8-14):

$$\alpha = 1.09 \left[\frac{32}{(6.02 \times 10^{23}) 1.14} \right]^3 = 14.2 \times 10^{-16} \text{ cm}^2$$

With this value of α the area equation [Eq. (8-13)] becomes

$$S_g = \frac{v_m(6.02 \times 10^{23})}{22,400} 14.2 \times 10^{-16} = 3.8 \times 10^4 v_m \text{ cm}^2/\text{g}$$

From curve 4 of Fig. (8-4),

$$I = 0.40 \times 10^{-3} \text{ cm}^{-3}$$

$$s = \frac{(5.4 - 0.4) \times 10^{-3}}{0.38 - 0} = 13.2 \times 10^{-3} \text{ cm}^{-3}$$

Then the monomolecular volume per gram of silica gel is, from Eq. (8-12),

$$v_m = \frac{10^3}{0.4 + 13.2} \frac{1}{0.606} = 122 \text{ cm}^3/\text{g catalyst}$$

Finally, substituting this value of v_m in the area expression gives

$$S_g = 3.8 \times 10^4 (122) = 465 \times 10^4 \text{ cm}^2/\text{g} \quad \text{or } 465 \text{ m}^2/\text{g}$$

The difference in area determined from the N_2 and O_2 data is somewhat larger than expected for these gases. The adsorption curve for N_2 at -183°C gives a value in closer agreement with $550 \text{ m}^2/\text{g}$ (see Prob. 8-1).

8-6 Void Volume and Solid Density

The void volume, or pore volume, of a catalyst particle can be estimated by boiling a weighed sample immersed in a liquid such as water. After the air in the pores has been displaced, the sample is superficially dried and weighed. The increase in weight divided by the density of the liquid gives the pore volume.

A more accurate procedure is the *helium-mercury method*. The volume of helium displaced by a sample of catalyst is measured; then the helium is removed, and the volume of mercury displaced is measured. Since mercury will not fill the pores of most catalysts at atmospheric pressure, the difference in volumes gives the pore volume of the catalyst sample. The volume of helium displaced is a measure of the volume occupied by the solid material. From this and the weight of the sample, the density of the solid phase, ρ_s , can be obtained. Then the void fraction, or porosity, of the particle, ϵ_p , may be calculated from the equation

$$\begin{aligned}\epsilon_p &= \frac{\text{void (pore) volume of particle}}{\text{total volume of particle}} = \frac{m_p V_g}{m_p V_g + m_p (1/\rho_s)} \\ &= \frac{V_g \rho_s}{V_g \rho_s + 1}\end{aligned}\quad (8-16)$$

where m_p is the mass of the particle and V_g is the void volume per gram of particles. If the sample of particles is weighed, the mass divided by the mercury volume gives the density of the porous particles. Note that the porosity is also obtainable from the density by the expression

$$\epsilon_p = \frac{\text{void volume}}{\text{total volume}} = \frac{V_g}{1/\rho_p} = \rho_p V_g \quad (8-17)$$

From the helium-mercury measurements the pore volume, the solid density, and the porosity of the catalyst particle can be determined. Values of ϵ_p are of the order of 0.5, indicating that the particle is about half void space and half solid material. Since overall void fractions in packed beds are about 0.4, a rule of thumb for a fixed-bed catalytic reactor is that about 30% of the volume is pore space, 30% is solid catalyst and carrier, and 40% is void space between catalyst particles. Individual catalysts may show results considerably different from these average values, as indicated in Examples 8-4 and 8-5.

Example 8-4 In an experiment to determine the pore volume and catalyst-particle porosity the following data were obtained on a sample of activated silica (granular, 4 to 12 mesh size):

Mass of catalyst sample placed in chamber = 101.5 g
 Volume of helium displaced by sample = 45.1 cm³
 Volume of mercury displaced by sample = 82.7 cm³

Calculate the required properties.

Solution The volume of mercury displaced, minus the helium-displacement volume, is the pore volume. Hence

$$V_g = \frac{82.7 - 45.1}{101.5} = 0.371 \text{ cm}^3/\text{g}$$

The helium volume is also a measure of the density of the solid material in the catalyst; that is,

$$\rho_s = \frac{101.5}{45.1} = 2.25 \text{ g/cm}^3$$

Substituting the values of V_g and ρ_s in Eq. (8-16) gives the porosity of the silica gel particles,

$$\epsilon_p = \frac{0.371(2.25)}{0.371(2.25) + 1} = 0.455$$

To avoid excessive pressure drops and improve mechanical strength, porous particles often must be pelleted to sizes of $\frac{1}{16}$ to 1 in. Usually the pellets are cylindrical, although spherical and granular assemblies are sometimes used. Agglomeration of porous particles gives a pellet containing two void regions: small void spaces within the individual particles and larger spaces between particles. Hence such materials are said to contain *bidisperse pore systems*. Although the shape and nature of these two void regions may vary from thin cracks to a continuous region surrounding a group of particles, it has been customary to designate both regions as *pores*. The void spaces within the particles are commonly termed *micropores*, and the void regions between particles are called *macropores*. *Particle* refers only to the small individual unit from which the pellet is produced. We shall use this nomenclature in discussing solid catalysts.

Not all catalyst supports can be agglomerized. Perhaps the most widely used pellets are those of alumina. Porous alumina particles (20 to 200 microns diameter) containing micropores of 10 to 200 Å diameter are readily prepared by spray drying. These somewhat soft particles are easily made into pellets. The macroporosity and macropore diameter depend on the pelleting pressure and can be varied over a wide range. Table 8-3 shows macro and micro properties of five alumina pellets, each prepared at a different pelleting pressure. The pellet density listed in the second column is approximately proportional to the pressure used. Comparison of the least and greatest pellet density shows that the macropore volume has decreased from 0.670 to 0.120 with increased pelleting pressure, while the micropore volume has decreased only from 0.434 to 0.365.

Table 8-3 Physical properties of alumina pellets

Density, g/cm ³		Pore volume, cm ³ /g		Void fraction		
Particle	Pellet	Micro	Macro	Total	Macro	Micro
1.292	1.121	0.365	0.120	0.543	0.134	0.409
1.264	1.010	0.383	0.198	0.587	0.200	0.387
1.238	0.896	0.400	0.308	0.634	0.275	0.359
1.212	0.785	0.416	0.451	0.680	0.353	0.327
1.188	0.672	0.434	0.670	0.725	0.450	0.275

NOTES: All properties are based on Al₂O₃. Micro refers to pore radii less than 100 Å, and macro refers to radii greater than 100 Å.

SOURCE: R. A. Mischke and J. M. Smith, *Ind. Eng. Chem., Fund. Quart.*, **1**, 288 (1962).

The external surface area of even very fine particles has been shown (Example 8-1) to be small with respect to the internal surface of the pores. Hence, in a catalyst pellet the surface resides predominantly in the small pores within the particles. The external surface of the particles, and of course the external area of the pellets, is negligible.

Macro- and micropore volumes and porosities for bidisperse catalyst pellets are calculated by the same methods as used for monodisperse pore systems. Example 8-5 illustrates the procedure.

Example 8-5 A hydrogenation catalyst is prepared by soaking alumina particles (100 to 150 mesh size) in aqueous NiNO_3 solution. After drying and reduction, the particles contain about 7 wt % NiO. This catalyst is then made into large cylindrical pellets for rate studies. The gross measurements for one pellet are

$$\begin{aligned}\text{Mass} &= 3.15 \text{ g} \\ \text{Diameter} &= 1.00 \text{ in.} \\ \text{Thickness} &= \frac{1}{4} \text{ in.} \\ \text{Volume} &= 3.22 \text{ cm}^3\end{aligned}$$

The Al_2O_3 particles contain micropores, and the pelleting process introduces macropores surrounding the particles. From the experimental methods already described, the macropore volume of the pellet is 0.645 cm^3 and the micropore volume is $0.40 \text{ cm}^3/\text{g}$ of particles. From this information calculate:

- The density of the pellet
- The macropore volume in cubic centimeters per gram
- The macropore void fraction in the pellet
- The micropore void fraction in the pellet
- The solid fraction
- The density of the particles
- The density of the solid phase
- The void fraction of the particles

Solution

- The density of the pellet is

$$\rho_P = \frac{3.15}{3.22} = 0.978 \text{ g/cm}^3$$

- The macropore volume per gram is

$$(V_g)_M = \frac{0.645}{3.15} = 0.205 \text{ cm}^3/\text{g}$$

- The macropore void fraction ϵ_M is obtained by applying Eq. (8-17) to the pellet. Thus

$$\epsilon_M = \frac{\text{macropore volume}}{\text{total volume}} = \frac{(V_g)_M}{1/\rho_P} = \frac{0.205}{1/0.978} = 0.200$$

(d) Since

$$(V_g)_\mu = 0.40 \text{ cm}^3/\text{g}$$

the micropore void fraction ϵ_μ in the pellet is

$$\epsilon_\mu = \frac{(V_g)_\mu}{1/\rho_p} = \frac{0.40}{1/0.978} = 0.391$$

(e) The solids fraction ϵ_s is given by

$$1 = \epsilon_M + \epsilon_\mu + \epsilon_s$$

$$\epsilon_s = 1 - 0.200 - 0.391 = 0.409$$

(f) The density ρ_p of the particles can be calculated by correcting the total volume of the pellet for the macropore volume. Thus

$$\rho_p = \frac{3.15}{3.22 - 0.645} = 1.22 \text{ g/cm}^3$$

or, in terms of 1 g of pellet,

$$\rho_p = \frac{1}{1/\rho_p - (V_g)_M} = \frac{\rho_p}{1 - (V_g)_M \rho_p}$$

$$\rho_p = \frac{0.978}{1 - 0.205(0.978)} = 1.22 \text{ g/cm}^3$$

(g) The density of the solid phase is

$$\begin{aligned} \rho_s &= \frac{\text{mass of pellet}}{(\text{volume of pellet}) \epsilon_s} \\ &= \frac{\rho_p}{\epsilon_s} = \frac{0.978}{0.409} = 2.39 \text{ g/cm}^3 \end{aligned}$$

(h) The void fraction of the particles is given by

$$\begin{aligned} \epsilon_p &= \frac{(V_g)_\mu}{1/\rho_p} = \rho_p (V_g)_\mu \\ &= 1.22(0.40) = 0.49 \end{aligned}$$

For this pellet a fraction equal to $\epsilon_M + \epsilon_\mu = 0.591$ is void and 0.409 is solid. Of the individual particles, a fraction 0.49 is void. Note that all these results were calculated from the mass and volume of the pellet and the measurements of macro- and micropore volumes.

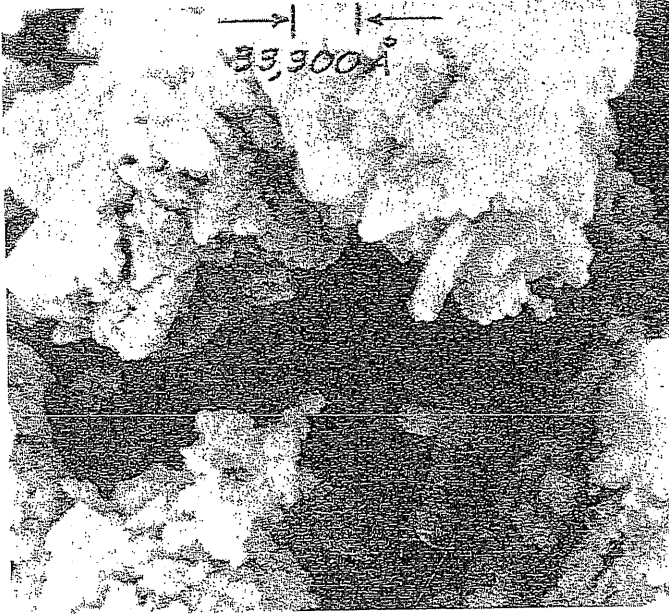
8-7 Pore-volume Distribution

We shall see in Chap. 11 that the effectiveness of the internal surface for catalytic reactions can depend not only on the extent of the void spaces

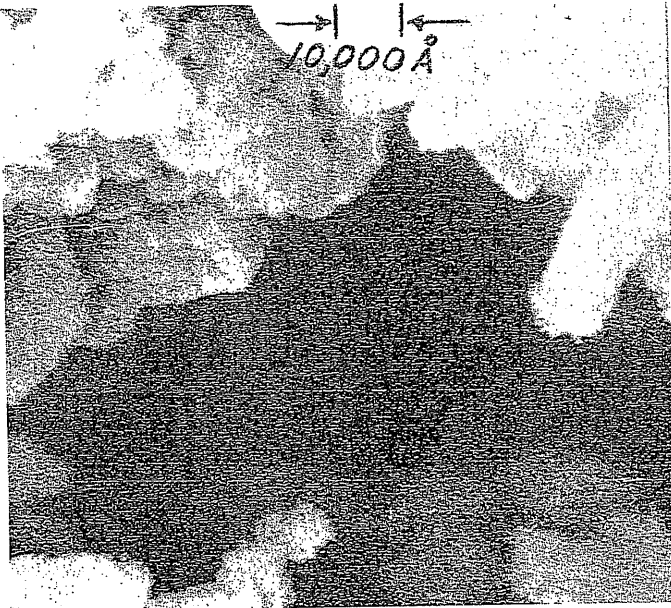
(V_g), but also on the size of the openings. Therefore it is desirable to know the distribution of void volume in a catalyst according to size of the opening. This is a difficult problem because the void spaces in a given particle are non uniform in size, shape, and length, and normally are interconnected. Further, these characteristics can change radically from one type of catalyst particle to another. Figure 8-5 shows electron-microscope (scanning type) photographs of porous silver particles ($S_g = 19.7 \text{ m}^2/\text{g}$). The material was prepared by reducing a precipitate of silver fumarate by heating at 350°C in a stream of nitrogen. The larger darker regions probably represent void space between individual particles, and the smaller dark spaces are intraparticle voids. The light portions are solid silver. The complex and random geometry shows that it is not very realistic to describe the void spaces as pores. It is anticipated that other highly porous materials such as alumina and silica would have similar continuous and complex void phases. For a material such as Vycor, with its relatively low porosity (0.3) and continuous solid phase, the concept of void spaces as pores is more reasonable.

In view of evidence such as that in Fig. 8-5, it is unlikely that detailed quantitative descriptions of the void structure of solid catalysts will become available. Therefore, to account quantitatively for the variations in rate of reaction with location within a porous catalyst particle, a simplified model of the pore structure is necessary. The model must be such that diffusion rates of reactants through the void spaces into the interior surface can be evaluated. More is said about these models in Chap. 11. It is sufficient here to note that in all the widely used models the void spaces are simulated as cylindrical pores. Hence the size of the void space is interpreted as a radius a of a cylindrical pore, and the distribution of void volume is defined in terms of this variable. However, as the example of the silver catalyst indicates, this does not mean that the void spaces are well-defined cylindrical pores.

There are two established methods for measuring the distribution of pore volumes. The mercury-penetration method depends on the fact that mercury has a significant surface tension and does not wet most catalytic surfaces. This means that the pressure required to force mercury into the pores depends on the pore radius. The pressure varies inversely with a ; 100 psi (approximately) is required to fill pores for which $a = 10,000 \text{ \AA}$, and 10,000 psi is needed for $a = 100 \text{ \AA}$. Simple techniques and equipment are satisfactory for evaluating the pore-volume distribution down to 100 to 200 \AA , but special high-pressure apparatus is necessary to go below $a = 100 \text{ \AA}$, where much of the surface resides. In the second method, the nitrogen-adsorption experiment (described in Sec. 8-5 for surface area measurement) is continued until the nitrogen pressure approaches the



(a)



(b)

Fig. 8-5 Electron micrographs of porous silver particles (approximate surface area = $19.7 \text{ m}^2/\text{g}$): (a) magnification = 3,000 (1 cm = 33,300 Å), (b) magnification = 10,000 (1 cm = 10,000 Å)

saturation value (1 atm at the normal boiling point). At $p/p_0 \rightarrow 1.0$, where p_0 is the saturation pressure, all the void volume is filled with adsorbed and condensed nitrogen. Then a desorption isotherm is established by lowering the pressure in increments and measuring the amount of nitrogen evaporated and desorbed for each increment. Since the vapor pressure of a liquid evaporating from a capillary depends on the radius of the capillary, these data can be plotted as volume desorbed vs pore radius. Thus this procedure also gives the distribution of pore volumes. Since the vapor pressure is not affected significantly by radii of curvature greater than about 200 Å, this method is not suitable for pores larger than 200 Å.

A combination of the two methods is normally necessary to cover the entire range of pore radii (10 to 10,000 Å) which may exist in a bidisperse catalyst or support, such as alumina pellets. For a monodisperse pore distribution, such as that in silica gel, the nitrogen-desorption experiment is sufficient, since there are few pores of radius greater than 200 Å. In a bidisperse pore system the predominant part of the catalytic reaction occurs in pores less than about 200 Å (the micropore region), since that is where the bulk of the surface resides. However, the transport of reactants to these small pores occurs primarily in pores of 200 to 10,000 Å (the macropore region). Hence the complete distribution of pore volume is necessary to establish the effectiveness of the interior surface, that is, the global rate of reaction. Calculation procedures and typical results are discussed briefly in the following paragraphs.

Mercury-penetration Method By equating the force due to surface tension (which tends to keep mercury out of a pore) to the applied force, Ritter and Drake¹ obtained

$$\pi a^2 p = -2\pi a \sigma \cos \theta$$

or

$$a = \frac{-2\sigma \cos \theta}{p} \quad (8-18)$$

where θ is the contact angle between the mercury and pore wall (Fig. 8-6). While θ probably varies somewhat with the nature of the solid surface, 140° appears to be a good average value. Then the working equation for evaluating the radius corresponding to a given pressure is

$$a(\text{Å}) = \frac{8.75 \times 10^5}{p \text{ (psi)}} \quad (8-19)$$

¹H. L. Ritter and L. C. Drake, *Ind. Eng. Chem., Anal. Ed.*, 17, 787 (1945).

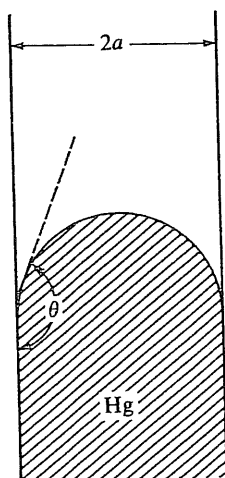


Fig. 8-6 Mercury penetration in a pore of radius a

Calculation of the pore-size distribution by this method is illustrated in Example 8-6.

Example 8-6 The mercury-penetration data given in Table 8-4 were obtained on a 0.624-g sample of a uranium dioxide pellet formed by sintering particles at 1000°C for 2 hr. Since the particles were nonporous, the void space was entirely between the

Table 8-4 Mercury porosimeter data for uranium dioxide pellet (mass of sample 0.624 g)

Pressure, psi	Mercury penetration, cm^3	Penetration, cm^3/g	
116	0.002	0.003	0.196
310	0.006	0.010	0.189
344	0.010	0.016	0.183
364	0.014	0.022	0.177
410	0.020	0.032	0.167
456	0.026	0.042	0.157
484	0.030	0.048	0.151
540	0.038	0.061	0.138
620	0.050	0.080	0.119
710	0.064	0.102	0.097
800	0.076	0.122	0.077
830	0.080	0.128	0.071
900	0.088	0.141	0.058
1,050	0.110	0.160	0.039
1,300	0.112	0.179	0.020
1,540	0.118	0.189	0.010
1,900	0.122	0.196	0.003
2,320	0.124	0.198	0.001
3,500	0.125	0.199	0

particles (macropores). At the beginning of the experiment (when the pressure was 1.77 psia) the amount of mercury displaced by the sample was found to be 0.190 cm³. Calculate the porosity and pore-volume distribution of the pellet.

Solution. According to Eq. (8-19), at $p = 1.77$ psia only pores larger than about 500,000 Å (50 microns) would be filled with mercury. No pores larger than this are likely. Hence 0.190 cm³ is the total volume of the sample. At the highest pressure, 3,500 psia, only pores less than $a = 250$ Å would remain unfilled. Since the pores were entirely of the macro type, few pores smaller 250 Å are expected. If such pores are neglected, the porosity can be calculated from the porosimeter measurements alone. Thus

$$\epsilon_p = \frac{0.125}{0.190} = 0.66$$

A check on this result is available from air-pycnometer¹ data, which gave a solid volume of 0.0565 cm³. Thus the total porosity is

$$(\epsilon_p)_t = \frac{0.190 - 0.0565}{0.190} = 0.70$$

The difference between values suggests that there were a few pores smaller than 250 Å in the sample, although the comparison also includes experimental errors in the two methods.

To calculate the pore-volume distribution the penetration data are first corrected to a basis of 1 g of sample, as given in the third column of Table 8-4. If we neglect the pores smaller than 250 Å, the penetration data can be reversed, starting with $V = 0$ at 3,500 psia (250 Å). The last column shows these figures. Then, from Eq. (8-19) and the pressure, the radius corresponding to each penetration value can be established. This gives the penetration curve shown in Fig. 8-7. The penetration volume at any pore radius a is the volume of pores larger than a . The derivative of this curve, $\Delta V/\Delta a$, is the volume of pores between a and $a + \Delta a$ divided by Δa ; that is, it is the distribution function for the pore volume according to pore radius. It is customary to plot the pore radius on a logarithmic coordinate as shown. Hence the distribution function is taken as the derivative of the curve so plotted, that is, $dV/d(\log a)$. The distribution function is also shown plotted against a in Fig. 8-7.

For this pellet the distribution is seen to be reasonably symmetrical with most of the volume in pores from 300 to 8,000 Å and with a most probable pore radius of 1,200 Å. Note that the flatness of the penetration curve at low pore radii justifies neglecting the pores smaller than 250 Å.

Wheeler² has summarized the assumptions and accuracy of the mercury-penetration method. It is important to note that erroneous results would be obtained if the porous particle contains large void spaces that are

¹ A device which uses air at two pressures to measure void volumes of porous materials. It provides the same data as the helium measurement described in Sec. 8-6.

² A. Wheeler, in P. H. Emmett (ed.), "Catalysis," vol. II, p. 123, Reinhold Publishing Corporation, New York, 1955.

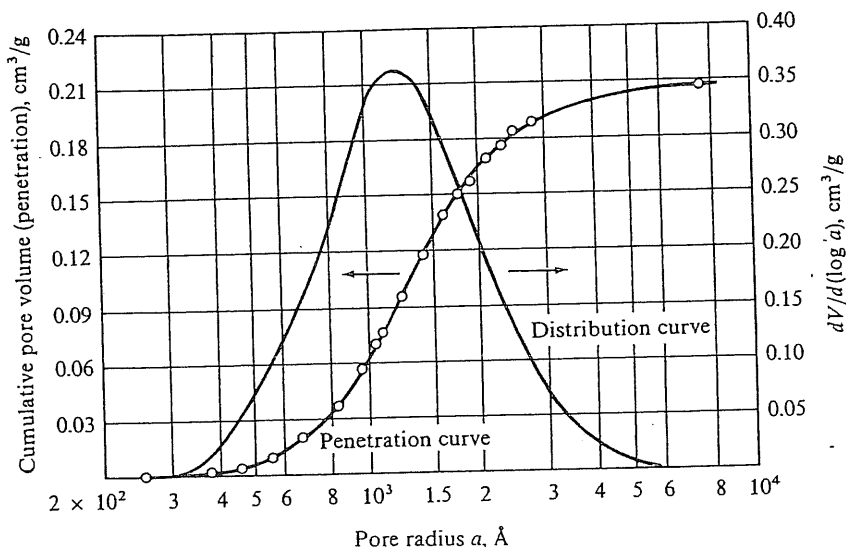


Fig. 8-7 Pore-volume distribution in a UO_2 pellet

connected only to smaller void spaces. Such “bottleneck” pores would fill with mercury at the higher pressure corresponding to the connecting smaller pores. For accurate results each porous region must be connected to at least one larger pore.

Nitrogen-desorption Method As the low-temperature nitrogen-adsorption experiment (Sec. 8-5) is continued to higher pressures multilayer adsorption occurs, and ultimately the adsorbed films are thick enough to bridge the pore.¹ Then further uptake of nitrogen will result in capillary condensation. Since the vapor pressure decreases as the capillary size decreases, such condensation will occur first in the smaller pores. Condensation will be complete, as $p/p_0 \rightarrow 1.0$, when the entire void region is filled with condensed nitrogen. Now, if the pressure is reduced by a small increment, a small amount of nitrogen will evaporate from the meniscus formed at the ends of the largest pores. Pores which are emptied of condensate in this way will be those in which the vapor pressure of nitrogen is greater than the chosen pressure. The Kelvin equation gives the relationship between vapor pressure and radius of the concave surface of the meniscus of the liquid. Since some of the nitrogen is adsorbed on the surface, and therefore not present because of capillary condensation, the Kelvin relationship must be corrected for the thickness δ of the adsorbed layers. With this correction, the pore radius is

¹L. H. Cohan, *J. Am. Chem. Soc.*, 60, 433 (1938); A. G. Foster, *J. Phys. Colloid Chem.*, 55, 638 (1951).

related to the saturation-pressure ratio (vapor pressure in the pore p divided by the normal vapor pressure p_0) by

$$a - \delta = \frac{-2\sigma V_l \cos \theta}{R_g T \ln(p/p_0)} \quad (8-20)$$

where V_l = molal volume of the condensed liquid

σ = surface tension

θ = contact angle between surface and condensate

Since nitrogen completely wets the surface covered with adsorbed nitrogen, $\theta = 0^\circ$ and $\cos \theta = 1$. The thickness δ depends on p/p_0 . The exact relationship has been the subject of considerable study,¹ but Halsey's form

$$\delta = A \left(\ln \frac{p_0}{p} \right)^{-1/n} \quad (8-21)$$

where A and n depend on the nature of the catalyst surface, is generally used.

For nitrogen at -195.8°C (normal boiling point) Eq. (8-20), for $a - \delta$ in Angstroms, becomes

$$a - \delta = 9.52 \left(\log \frac{p_0}{p} \right)^{-1} \quad (8-22)$$

Wheeler proposes for Eq. (8-21)

$$\delta (\text{\AA}) = 7.34 \left(\ln \frac{p_0}{p} \right)^{-1/3} \quad (8-23)$$

For a chosen value of p/p_0 , Eqs. (8-22) and (8-23) give the pore radius above which all pores will be empty of capillary condensate. Hence, if the amount of desorption is measured for various p/p_0 , the pore volume corresponding to various radii can be evaluated. Differentiation of the curve for cumulative pore volume vs radius gives the distribution of volume as described in Example 8-6. Descriptions of the method of computation are given by several investigators.² As in the mercury-penetration method, errors will result unless each pore is connected to at least one larger pore.

Figure 8-8 shows the result of applying the method to a sample of Vycor (porous glass).³ This material, which contained only micropores, had the properties

¹A. Wheeler, in P. H. Emmett (ed.), "Catalysis," vol. II, chap. 2, Reinhold Publishing Corporation, New York, 1955; G. D. Halsey, *J. Chem. Phys.*, **16**, 931 (1948); C. G. Shull, *J. Am. Chem. Soc.*, **70**, 1405 (1948); J. O. Mingle and J. M. Smith, *Chem. Eng. Sci.*, **16**, 31 (1961).

²E. P. Barrett, L. G. Joyner, and P. P. Halenda, *J. Am. Chem. Soc.*, **73**, 373 (1951); C. J. Pierce, *J. Phys. Chem.*, **57**, 149 (1953); R. B. Anderson, *J. Catalysis*, **3**, 50 (1964).

³M. R. Rao and J. M. Smith, *AIChE J.*, **10**, 293 (1964).

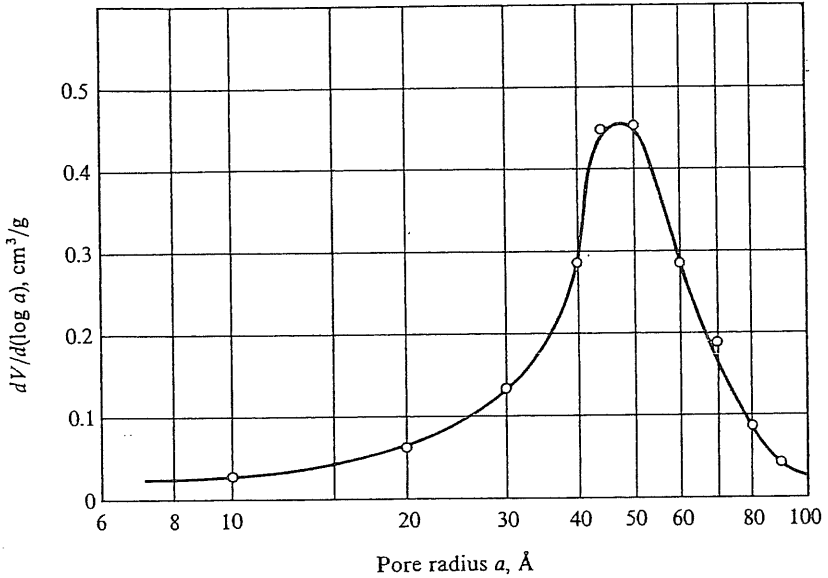
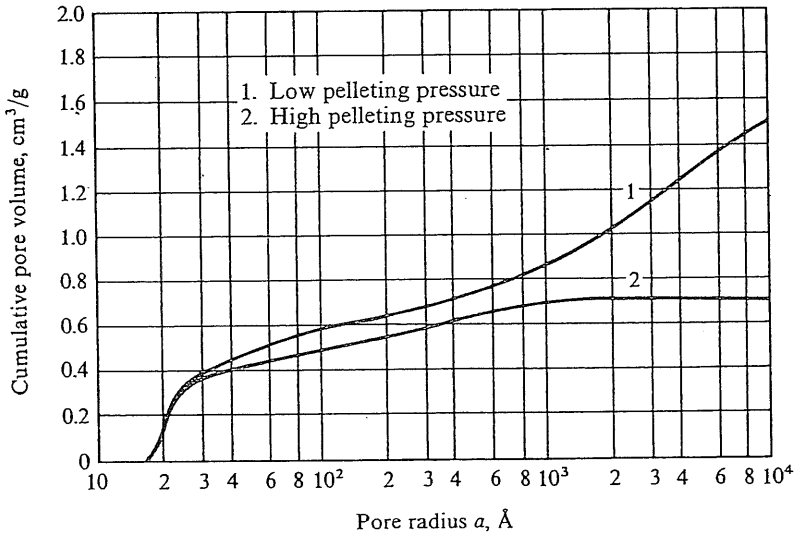


Fig. 8-8 Pore-volume distribution in Vycor; $\rho_p = 1.46 \text{ g/cm}^3$, $V_g = 0.208 \text{ cm}^3/\text{g}$, $S_g = 90 \text{ m}^2/\text{g}$

Fig. 8-9 Pore volume in alumina (boehmite) pellets



$$\rho_p = 1.46 \text{ g/cm}^3$$

$$V_g = 0.208 \text{ cm}^3/\text{g}$$

$$\epsilon_p = 0.304$$

$$S_g = 90 \text{ m}^2/\text{g}$$

The surface area was determined from nitrogen-adsorption data in the low p/p_0 range, as described in Sec. 8-5, while the distribution results in Fig. 8-8 were established from the desorption curve in the capillary-condensation (high p/p_0) region.

By combining mercury-penetration and nitrogen-desorption measurements, pore-volume information can be obtained over the complete range of radii in a pelleted catalyst containing both macro- and micropores. Figure 8-9 shows the cumulative pore volume for two alumina pellets, each prepared by compressing porous particles of boehmite ($\text{Al}_2\text{O}_3 \cdot \text{H}_2\text{O}$). The properties¹ of the two pellets are given in Table 8-5. The only difference in the two is the pelleting pressure. Increasing this pressure causes drastic reductions in the space between particles (macropore volume) but does not greatly change the void volume within the particles or the surface area. The derivative of the volume curves in Fig. 8-9 gives the pore-volume distribution, and these results are shown in Fig. 8-10. In this figure the bidisperse pore system, characteristic of alumina pellets, is clearly indicated. The micropore range within the particles is narrow, with a most probable

¹The properties and pore-volume distribution were determined by M. F. L. Johnson, Sinclair Research Laboratories, Harvey, Ill., by the methods described in Secs. 8-5 to 8-7. They were originally reported in J. L. Robertson and J. M. Smith, *AIChE J.*, 9, 344 (1963).

Fig. 8-10 Pore-volume distribution in alumina pellets

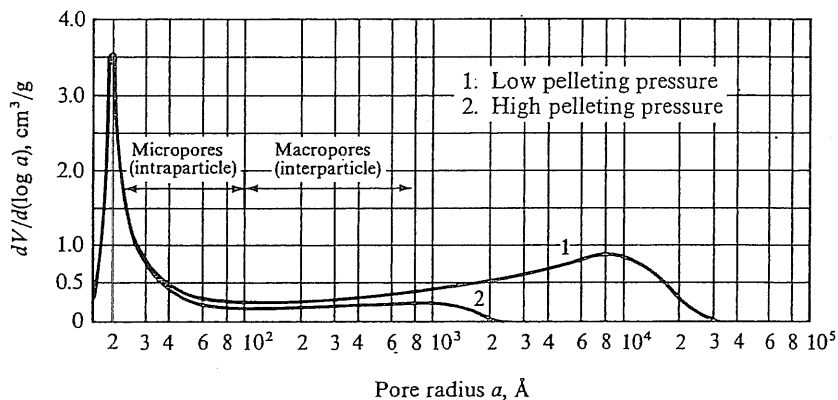


Table 8-5 Properties of boehmite ($Al_2O_3 \cdot H_2O$) pellets

Pelleting pressure	Macropore volume, cm^3/g	Micropore volume, cm^3/g	Surface area, m^2/g
Low	1.08	0.56	389
High	0.265	0.49	381

NOTES: Volume and surface area refer to mass of Al_2O_3 obtained by ignition of boehmite. The pore-volume distribution is given in Fig. 8-10. Average particle size from which pellets were made was 85 microns.

radius of 20 Å. The macropores cover a much wider range of radii and show the effect of pelleting pressure. For the high-pressure pellet all volume with pores greater than 2,000 Å has been squeezed out, while the most probable radius for the low-pressure pellet is 8,000 Å. Pelleting pressure seems to have little effect on the micropores, which suggests that the particles themselves are not crushed significantly during the pelleting process.

Some models (see Chap. 11) for quantitative treatment of the effectiveness of the internal catalyst surface require only the average pore radius \bar{a} , rather than the distribution of pore volumes. Wheeler¹ has developed a simple equation for \bar{a} which requires only surface-area and pore-volume measurements. Suppose all the pores in a hypothetical particle are straight, cylindrical, not interconnected, and have the same radius \bar{r} and length \bar{L} . The average pore radius may be found by writing equations for the total surface and volume in the hypothetical particle and equating these quantities to the surface $m_p S_g$ and volume $m_p V_g$ in the actual particle; i.e.

$$m_p S_g = (2\pi\bar{a}\bar{L})n \quad (8-24)$$

$$m_p V_g = (\pi\bar{a}^2\bar{L})n \quad (8-25)$$

where m_p and n are the mass and number of pores per particle. Dividing the two equations gives the Wheeler average pore radius,

$$\bar{a} = \frac{2V_g}{S_g} \quad (8-26)$$

This expression agrees well with volume-average values obtained from the distribution curve for monodisperse pore systems. For example, from the data for the Vycor sample (Fig. 8-7) Eq. (8-26) gives

$$\bar{a} = \frac{2(0.208)}{90 \times 10^4} = 46 \times 10^{-8} \text{ cm} \quad \text{or } 46 \text{ \AA}$$

¹A. Wheeler, in P. H. Emmett (ed.), "Catalysis," vol. II, chap. 2, Reinhold Publishing Corporation, New York, 1955.

The volume-average value is calculated from the pore volume data used to obtain the distribution curve (Fig. 8-8) and the expression

$$\bar{a} \doteq \frac{\int_0^{V_g} a dV}{V_g}$$

By this method $\bar{a} = 45 \text{ \AA}$.

Accurate values of the small areas existing in macropore systems make it difficult to use Eq. (8-26) to calculate \bar{a} for interparticle pores. Hence the average radius for systems such as the UO_2 pellets discussed in Example 8-6 should be obtained by integrating under the cumulative-volume-vs- \bar{a} curve shown in Fig. 8-7. Also a single value of \bar{a} has no meaning for a bidisperse pore system such as that in an alumina pellet. Thus using the total pore volume in Table 8-5 for the low-pressure pellet gives

$$\bar{a} = \frac{2(1.64)}{389 \times 10^4} = 84 \times 10^{-8} \text{ cm} \quad \text{or } 84 \text{ \AA}$$

As Fig. 8-10 shows, there is very little pore volume (very few pores) in this radius region. If Eq. (8-26) is applied to the micropore region, arbitrarily taken as pores smaller than $a = 100 \text{ \AA}$,

$$\bar{a}_\mu = \frac{2(0.56)}{389 \times 10^4} = 29 \times 10^{-8} \text{ cm} \quad \text{or } 29 \text{ \AA}$$

Figure 8-10 shows that this is an approximate value for the *average* pore radius in the micropore region. Note that the micropore distribution is asymmetrical in such a way that the average radius is greater than the most probable value (20 \AA).

Summary In concluding the treatment of physical properties of catalysts, let us review the purpose for studying properties and structure of porous solids. Heterogeneous reactions with solid catalysts occur on parts of the surface active for chemisorption. The number of these active sites and the rate of reaction is, in general, proportional to the extent of the surface. Hence it is necessary to know the surface area. This is evaluated by low-temperature-adsorption experiments in the pressure range where a monomolecular layer of gas (usually nitrogen) is physically adsorbed on the catalyst surface. The effectiveness of the interior surface of a particle (and essentially all of the surface is in the interior) depends on the volume and size of the void spaces. The pore volume (and porosity) can be obtained by simple pycnometer-type measurements (see Examples 8-4 and 8-5). The average size (pore radius) can be estimated by Eq. (8-26) from the

surface area and pore volume in some *monodisperse* systems. Determination of the complete distribution of pore volume according to pore radius requires either mercury-penetration measurements or nitrogen-adsorption data at pressures where capillary condensation occurs, or both. Accurate values of the mean pore radius can be evaluated from such pore-volume-vs-radius data. Note also that a measurement of the complete nitrogen-adsorption-desorption isotherm is sufficient to calculate surface area and pore volume, and distribution of pore sizes, in the range $10 \text{ \AA} < a < 200 \text{ \AA}$.

CLASSIFICATION AND PREPARATION OF CATALYSTS

8-8 Classification of Catalysts

In discussing catalysis it is well to recall proposals concerning what factors are important in making solids active as catalysts. In chronological order, Sabatier¹ suggested that a mechanism for the activity of nickel as a hydrogenation catalyst might involve formation of a chemical compound, nickel hydride. Since then, the *chemical factor* continues to be recognized as important. Later Taylor,² Balandin,³ and Beeck⁴ provided evidence for the significance of *geometric properties*. According to this concept the catalytic activity of a solid surface depends on the spacing of atoms so as to facilitate adsorption of reactant molecules. Over the years most of the evidence for the geometric theory has proved suspect, except that for metallic films. The work of Boudart⁵ and Beeck changed the emphasis from geometric considerations to *electronic properties*. In 1948 Dowden and coworkers⁶ proposed that catalysts might be classified, on the basis of electron mobility, as conductors, semiconductors, and insulators.

The conductor catalysts are the metals (silver, platinum, vanadium, iron, etc.) and have the property of chemisorption by electron transfer. The semiconductor catalysts are the oxides, such as NiO, Cu₂O, and ZnO. These materials have the capability of interchanging electrons from the filled valence bands in a compound when sufficient energy is provided,

¹P. Sabatier, "Catalysis in Organic Chemistry," trans. by E. E. Reid, in "Catalysis, Then and Now," Franklin Publishing Company, Englewood, N.J., 1965.

²H. S. Taylor, *Proc. Roy. Soc. (London)*, **A108**, 105 (1925).

³A. A. Balandin, "Advances in Catalysis," vol. X, p. 96, Academic Press, Inc., New York, 1958.

⁴O. Beeck, *Disc. Faraday Soc.*, **8**, 118 (1950).

⁵M. Boudart, *J. Am. Chem. Soc.*, **72**, 1040 (1950).

⁶D. A. Dowden, *Research*, **1**, 239 (1948); D. A. Dowden and P. W. Reynolds, *Disc. Faraday Soc.*, **8**, 187 (1950).

for example, by heating. Upon this electron transfer the semiconductor becomes a conductor.¹ The insulator catalysts include such widely used substances as silica gel, alumina, and their combinations. Even at high temperatures, electrons are not supposed to be able to move through these two solids freely enough to justify their being called conductors. These substances are also known to be strong acids. Their activity in the many hydrocarbon reactions which they catalyze is presumably due to the formation of carbonium ions at the acid sites on the surface. While much has been written about carbonium-ion mechanisms, the basic concepts are well described in the original work of Whitmore² and the later work of Greensfelder.³

It should be emphasized that the electronic theory is not without uncertainties and at present should be considered as a concept in transition.⁴ However, it does provide a convenient, and probably helpful, method of classifying solid catalysts.

Metals chemisorb oxygen and hydrogen and therefore are usually effective catalysts for oxidation-reduction and hydrogenation-dehydrogenation reactions. Thus platinum is a successful catalyst for the oxidation of SO₂, and Ni is used effectively for hydrogenation of hydrocarbons. The metal oxides, as semiconductors, catalyze the same kinds of reactions, but often higher temperatures are required. Because of the relative strength of the chemisorption bond with which such gases as O₂ and CO are attached to metals, these gases are poisons when metals are employed as hydrogenation catalysts. The semiconductor oxides are less susceptible to such poisoning. Oxides of the transition metals, such as MoO₃ and Cr₂O₃, are good catalysts for polymerization of olefins.

In connection with miscellaneous catalysts the work on polymerizing ethylene should be mentioned. It has been found⁵ that aluminum alkyl-

¹Semiconductors are classified as *p* type if they tend to attract electrons from the chemisorbed species, or as *n* type if they donate electrons to this species. The *p* type are normally the compounds, such as NiO. The *n* type are substances which contain small amounts of impurities, or the oxide is present in nonstoichiometric amounts (as, for example, when some of the zinc in ZnO has been reduced). Reviews of semiconductors as catalysts are given by P. H. Emmett ("New Approaches to the Study of Catalysis," 36th Annual Priestly Lectures, Pennsylvania State University, April 9-13, 1962) and by P. G. Ashmore ("Catalysis and Inhibition of Chemical Reactions," Butterworths & Co. (Publishers), London, 1963.

²F. C. Whitmore, *J. Am. Chem. Soc.*, **54**, 3274 (1932).

³B. S. Greensfelder, "Chemistry of Petroleum Hydrocarbons," vol. II, chap. 27, Reinhold Publishing Corporation, New York, 1955.

⁴An analysis of the electronic theory is given by Th. Volkenstein, in "Advances in Catalysis," vol. XII, p. 189, Academic Press Inc., New York, 1960.

⁵K. Ziegler, *Angew. Chem.*, **64**, 323 (1952); G. Natta and I. Pasquon, in "Advances in Catalysis," vol. XI, p. 1, Academic Press Inc., New York, 1959.

titanium chloride [for example, $\text{Al}(\text{C}_2\text{H}_5)_3 + \text{TiCl}_4$] constitutes an excellent catalyst for producing isotactic polymers from olefins. Alumina and silica catalysts are widely used for alkylation, isomerization, polymerization, and particularly for cracking of hydrocarbons. In each case the mechanism presumably involves carbonium ions formed at the acid sites on the catalyst. While the emphasis here has been on solid catalysts, liquid and gaseous acids, particularly H_2SO_4 and HF, are well-known alkylation and isomerization catalysts.

Often catalysts are specific. An important example is the effectiveness of iron for producing hydrocarbons from hydrogen and carbon monoxide (the Fischer-Tropsch synthesis). Dual-function catalysts for isomerization and reforming reactions consist of two active substances in close proximity to each other. For example, Ciapetta and Hunter¹ found that a silica-alumina catalyst upon which nickel was dispersed was much more effective in isomerizing *n*-hexane than silica alumina alone. The explanation depends on the fact that olefins are more readily isomerized than paraffin hydrocarbons. The nickel presumably acts as a hydrogenating agent, producing hexene, after which the silica alumina isomerizes the hexene to isohexene. Finally, the nickel is effective in hydrogenating hexene back to hexanes.

This discussion of catalysts for reaction types is general and superficial. Much has and is being written on the subject, and helpful sources of summary information are available.²

8-9 Catalyst Preparation

Experimental methods and techniques for catalyst manufacture are particularly important because chemical composition is not enough by itself to determine activity. The physical properties of surface area, pore size, particle size, and particle structure also have an influence. These properties are determined to a large extent by the preparation procedure. To begin with, a distinction should be drawn between preparations in which the entire material constitutes the catalyst and those in which the active ingredient is dispersed on a support or *carrier* having a large surface area. The first kind of catalyst is usually made by precipitation, gel formation, or simple mixing of the components.

Precipitation provides a method of obtaining the solid material in a porous form. It consists of adding a precipitating agent to aqueous solutions

¹F. G. Ciapetta and J. B. Hunter, *Ind. Eng. Chem.*, **45**, 155 (1953).

²P. H. Emmett (ed.), "Catalysis," Reinhold Publishing Corporation, New York, 1954-; "Advances in Catalysis," Academic Press Inc., New York, 1949-; *J. Catalysis*, **1**, 1962-; A. A. Balandin, "Scientific Selection of Catalysts," trans. by A. Aledjem, Davey Publishing Company, Hartford, Conn., 1968.

of the desired components. Washing, drying, and sometimes calcination and activation are subsequent steps in the process. For example, a magnesium oxide catalyst can be prepared by precipitating the magnesium from nitrate solution by adding sodium carbonate. The precipitate of $MgCO_3$ is washed, dried, and calcined to obtain the oxide. Such variables as concentration of the aqueous solutions, temperature, and time of the drying and calcining steps may influence the surface area and pore structure of the final product. This illustrates the difficulty in reproducing catalysts and indicates the necessity of carefully following tested recipes. Of particular importance is the washing step to remove all traces of impurities, which may act as poisons.

A special case of the precipitation method is the formation of a colloidal precipitate which gels. The steps in the process are essentially the same as for the usual precipitation procedure. Catalysts containing silica and alumina are especially suitable for preparation by gel formation, since their precipitates are of a colloidal nature. Detailed techniques for producing catalysts through gel formation or ordinary precipitation are given by Ciapetta and Plank.¹

In some instances a porous material can be obtained by mixing the components with water, milling to the desired grain size, drying, and calcining. Such materials must be ground and sieved to obtain the proper particle size. A mixed magnesium and calcium oxide catalyst can be prepared in this fashion. The carbonates are milled wet in a ball machine, extruded, dried, and reduced by heating in an oven.

Catalyst *carriers* provide a means of obtaining a large surface area with a small amount of active material. This is important when expensive agents such as platinum, rickel, and silver are used. Berkman et al.² have treated the subject of carriers in some detail.

The steps in the preparation of a catalyst impregnated on a carrier may include (1) evacuating the carrier, (2) contacting the carrier with the impregnating solution, (3) removing the excess solution, (4) drying, (5) calcination and activation. For example, a nickel hydrogenation catalyst can be prepared on alumina by soaking the evacuated alumina particles with nickel nitrate solution, draining to remove the excess solution, and heating in an oven to decompose the nitrate to nickel oxide. The final step, reduction of the oxide to metallic nickel, is best carried out with the particles in place in the reactor by passing hydrogen through the equipment. Activation *in situ* prevents contamination with air and other gases which might

¹F. G. Ciapetta and C. J. Plank, in P. H. Emmett (ed.), "Catalysis," vol I, chap. 7, Reinhold Publishing Corporation, New York, 1954.

²S. Berkman, J. C. Morrell, and G. Egloff, "Catalysis," Reinhold Publishing Corporation, New York, 1940.

poison the reactive nickel. In this case no precipitation was required. This is a desirable method of preparation, since thorough impregnation of all the interior surface of the carrier particles is relatively simple. However, if the solution used to soak the carrier contains potential poisons such as chlorides or sulfates, it may be necessary to precipitate the required constituent and wash out the possible poison.

The nature of the support can affect catalyst activity and selectivity. This effect presumably arises because the support can influence the surface structure of the atoms of dispersed catalytic agent. For example, changing from a silica to alumina carrier may change the electronic structure of deposited platinum atoms. This question is related to the optimum amount of catalyst that should be deposited on a carrier. When only a small fraction of a monomolecular layer is added, increases in amount of catalyst should increase the rate. However, it may not be helpful to add large amounts to the carrier. For example, the conversion rate of the ortho to para hydrogen with a NiO catalyst deposited on alumina was found¹ to be less for 5.0 wt % NiO than for 0.5 wt % NiO. The dispersion of the catalyst on the carrier may also be an important factor in such cases. The nickel particles were deposited from a much more concentrated NiNO₃ solution to make the catalyst containing 5.0 wt % NiO. This may have led to larger nickel particles. That is, many more nickel atoms were deposited on top of each other, so that the dispersion of nickel on the surface was less uniform than with the 0.5 wt % catalyst. It is interesting to note that a 5.0 wt % NiO catalyst prepared by 10 individual depositions of 0.5 wt % was much more active (by a factor of 11) than the 5.0 wt % added in a single treatment. This method gave a much larger active nickel surface, presumably because of better dispersion of the nickel atoms on the Al₂O₃ surface. Since the total amount of nickel was the same for the two preparations, one would conclude that the individual particles of nickel were smaller in the 10-application catalyst. These kinds of data indicate the importance of measuring surface areas for chemisorption of the reactants involved. A technique based on the chemisorption of H₂ and CO has been developed² to study the effect of dispersion of a catalyst on its activity and the effect of interaction between catalyst and support on activity.

8-10 Promoters and Inhibitors

As normally used, the term "catalyst" designates the composite product used in a reactor. Components of the catalyst must include the catalytically

¹N. Wakao, J. M. Smith, and P. W. Selwood, *J. Catalysis*, **1**, 62 (1962).

²G. K. Boreskov and A. P. Karnaukov, *Zh. Fiz. Khim.*, **26**, 1814 (1952); L. Spenadel and M. Boudart, *J. Phys. Chem.*, **64**, 204 (1960).

active substance itself and may also include a carrier, promoters, and inhibitors.

Innes¹ has defined a *promoter* as a substance added during the preparation of a catalyst which improves activity or selectivity or stabilizes the catalytic agent so as to prolong its life. The promoter is present in a small amount and by itself has little activity. There are various types, depending on how they act to improve the catalyst. Perhaps the most extensive studies of promoters has been in connection with iron catalysts for the ammonia synthesis reaction.² It was found that adding Al_2O_3 (other promoters are CaO , K_2O) prevented reduction (by sintering) in surface area during catalyst use and gave an increased activity over a longer period of time. Some promoters are also believed to increase the number of active centers and so make the existing catalyst surface more active. The published information on promoters is largely in the patent literature. Innes has tabulated the data appearing from 1942 to 1952.

An *inhibitor* is the opposite of a promoter. When added in small amounts during catalyst manufacture, it lessens activity, stability, or selectivity. Inhibitors are useful for reducing the activity of a catalyst for an undesirable side reaction. For example, silver supported on alumina is an excellent oxidation catalyst. In particular, it is used widely in the production of ethylene oxide from ethylene. However, at the same conditions complete oxidation to carbon dioxide and water also occurs, so that selectivity to $\text{C}_2\text{H}_4\text{O}$ is poor. It has been found that adding halogen compounds to the catalyst inhibits the complete oxidation and results in satisfactory selectivity.

8-11 Poisons (Catalyst Life)

In some systems the catalyst activity decreases so slowly that exchange for new material or regeneration is required only at long intervals. Examples are promoted catalysts for synthetic ammonia and catalysts containing metals such as platinum and silver. Catalysts for cracking and some other hydrocarbon reactions, however, require frequent regeneration. The decrease in activity is due to *poisons*, which will be defined here as substances, either in the reactants stream or produced by the reaction, which lower the activity of the catalyst. The frequent regeneration of cracking catalysts is necessary because of the deposition of one of the products, carbon, on the surface.

Poisons can be differentiated in terms of the way in which they operate. Many summaries listing specific poisons and classifying groups of poisons

¹W. B. Innes, in P. H. Emmett (ed.), "Catalysis," vol. 1, chap. 7, Reinhold Publishing Corporation, New York, 1954.

²P. H. Emmett and S. Brunauer, *J. Am. Chem. Soc.*, **62**, 1732 (1940).

are available.¹ The following arrangement has been taken in part from Innes.

DEPOSITED POISONS Carbon deposition on catalysts used in the petroleum industry falls into this category. The carbon covers the active sites of the catalyst and may also partially plug the pore entrances. This type of poisoning is at least partially reversible, and regeneration can be accomplished by burning to CO and CO₂ with air and/or steam. The regeneration process itself is a heterogeneous reaction, a gas-solid noncatalytic one. In the design of the reactor, attention must be given to the regeneration as well as to the reaction parts of the cycle. The quantitative description of the drop in activity with time during reaction and the increase in activity during regeneration has been investigated.²

CHEMISORBED POISONS Compounds of sulfur and other materials are frequently chemisorbed on nickel, copper, and platinum catalysts. The decline in activity stops when equilibrium is reached between the poison in the reactant stream and that on the catalyst surface. If the strength of the adsorption compound is low, the activity will be regained when the poison is removed from the reactants. If the adsorbed material is tightly held, the poisoning is more permanent. The mechanism appears to be one of covering the active sites, which could otherwise adsorb reactant molecules.

SELECTIVITY POISONS The selectivity of a solid surface for catalyzing one reaction with respect to another is not well understood. However, it is known that some materials in the reactant stream will adsorb on the surface and then catalyze other undesirable reactions, thus lowering the selectivity. The very small quantities of nickel, copper, iron, etc., in petroleum stocks may act as poisons in this way. When such stocks are cracked, the metals deposit on the catalyst and act as dehydrogenation catalysts. This results in increased yields of hydrogen and coke and lower yields of gasoline.

STABILITY POISONS When water vapor is present in the sulfur dioxide-air mixture supplied to a platinum-alumina catalyst, a decrease in oxidation activity occurs. This type of poisoning is due to the effect of water on the structure of the alumina carrier. Temperature has a pronounced effect on

¹R. H. Griffith, "The Mechanism of Contact Catalysis," p. 93, Oxford University Press, New York, 1936; E. B. Maxted, *J. Soc. Chem. Ind. (London)*, 67, 93 (1948); P. H. Emmett (ed.), "Catalysis," vol. I, chap. 6, Reinhold Publishing Corporation, New York, 1954.

²Typical references are M. Sagara, S. Masamune, and J. M. Smith, *AIChE J.*, 13, 1226 (1967); G. F. Froment and K. B. Bischoff, *Chem. Eng. Sci.*, 16, 189 (1961); P. B. Weisz and R. D. Goodwin, *J. Catalysis*, 2, 397 (1963).

stability poisoning. Sintering and localized melting may occur as the temperature is increased, and this, of course, changes the catalyst structure.

DIFFUSION POISONS This kind of poisoning has already been mentioned in connection with carbon deposition on cracking catalysts. Blocking the pore mouths prevents the reactants from diffusing into the inner surface. Entrained solids in the reactants, or fluids which can react with the catalyst to form a solid residue, can cause this type of poisoning.

Table 8-6 lists poisons for various catalysts and reactions. The materials that are added to reactant streams to improve the performance of a catalyst are called *accelerators*. They are the counterparts of poisons. For example, steam added to the butene feed of a dehydrogenation reactor appeared to reduce the amount of coke formed and increase the yield of butadiene. The catalyst in this case was iron.¹

Table 8-6 Poisons for various catalysts

Catalyst	Reaction	Types of poisoning	Poisons
Silica, alumina	Cracking	Chemisorption Deposition Stability Selectivity	Organic bases Carbon, hydrocarbons Water Heavy metals
Nickel, platinum, copper	Hydrogenation Dehydrogenation 	Chemisorption	Compounds of S, Se, Te, P, As, Zn, halides, Hg, Pb, NH ₃ , C ₂ H ₂ , H ₂ S, Fe ₂ O ₃ , etc.
Cobalt	Hydrocracking	Chemisorption	NH ₃ , S, Se, Te, P
Silver	C ₂ H ₄ + O → C ₂ H ₄ O	Selectivity	CH ₄ , C ₂ H ₆
Vanadium oxide	Oxidation	Chemisorption	As
Iron	Ammonia synthesis Hydrogenation Oxidation	Chemisorption Chemisorption Chemisorption	O ₂ , H ₂ O, CO, S, C ₂ H ₂ Bi, Se, Te, P, H ₂ O VSO ₄ , Bi

SOURCE: In part from W. B. Innes in P. H. Emmett (ed), "Catalysis," vol. I, chap. 7, p. 306, Reinhold Publishing Corporation, New York, 1954.

Problems

8-1. The following data were obtained at 70°C for the equilibrium adsorption of *n*-hexane on silica gel particles ($S_g = 832 \text{ m}^2/\text{g}$, $c_p = 0.486$, $\rho_p = 1.13 \text{ g/cm}^3$, $V_g = 0.43 \text{ cm}^3/\text{g}$).

¹K. K. Kearly, *Ind. Eng. Chem.*, 42, 295 (1950).

Partial pressure of C_6H_{14} in gas, atm	C_6H_{14} adsorbed, g moles/(g gel)
0.0020	10.5×10^{-5}
0.0040	16.0×10^{-5}
0.0080	27.2×10^{-5}
0.0113	34.6×10^{-5}
0.0156	43.0×10^{-5}
0.0206	47.3×10^{-5}

(a) Determine how well the Langmuir isotherm fits these data. Establish the values of the constants \bar{C}_m and K_c by least-mean-squares analysis of the linearized form of Eq. (8-6):

$$\frac{C_g}{\bar{C}} = \frac{1}{K_c \bar{C}_m} + \frac{C_g}{\bar{C}_m}$$

Note that a straight line should be obtained if C_g/\bar{C} is plotted against C_g .

(b) Estimate the fraction of the surface covered with an adsorbed monomolecular layer at each partial pressure of *n*-hexane. The surface occupied by one molecule of hexane at 70°C is estimated to be 58.5×10^{-16} cm².

(c) Calculate the value of \bar{C}_m from the total surface area and the area occupied by one molecule of hexane. What conclusions can be drawn from the comparison of this value of \bar{C}_m with that obtained in part (a)? (d) Up to what gas concentration is the isotherm linear?

- 8-2. Repeat Prob. 8-1 for the following data for the equilibrium adsorption of C_6H_6 on the same silica gel at 110°C. The surface occupied by one benzene molecule is 34.8×10^{-16} cm².

Partial pressure of C_6H_6 in gas, atm	C_6H_6 adsorbed, g moles/(g gel)
5.0×10^{-4}	2.6×10^{-5}
1.0×10^{-3}	4.5×10^{-5}
2.0×10^{-3}	7.8×10^{-5}
5.0×10^{-3}	17.0×10^{-5}
1.0×10^{-2}	27.0×10^{-5}
2.0×10^{-2}	40.0×10^{-5}

- 8-3. Curve 3 of Fig. 8-4 is a Brunauer-Emmett-Teller plot for the adsorption data of N_2 at -183°C on the sample of silica gel. The density of liquid N_2 at this temperature is 0.751 g/cm³. Estimate the area of the silica gel from these data, in square meters per gram, and compare with the results of Example 8-2.
- 8-4. The "point-*B* method" of estimating surface areas was frequently used prior to the development of the Brunauer-Emmett-Teller approach. It entailed choosing from an absorption diagram such as Fig. 8-3 the point at which the central linear section begins. This procedure worked well for some systems, but it was extremely difficult, if not impossible, to select a reliable point *B* on an isotherm such as that shown for *n*-butane in Fig. 8-3. In contrast, the Brunauer-Emmett-Teller method was found to be reasonably satisfactory for this type of isotherm.

Demonstrate this by estimating the surface area of the silica gel sample from the *n*-butane curve in Fig. 8-4 (multiply the ordinate of the *n*-butane curve by 10). The density of liquid butane at 0°C is 0.601 g/cm³.

- 8-5. An 8.01-g sample of Glaucosil is studied with N₂ adsorption at -195.8°C. The following data are obtained:

Pressure, mm Hg	6	25	140	230	285	320	430	505
Volume adsorbed, cm ³ (at 0°C and 1 atm)	61	127	170	197	215	230	277	335

The vapor pressure of N₂ at -195.8°C is 1 atm. Estimate the surface area (square meters per gram) of the sample.

- 8-6. Low-temperature (-195.8°C) nitrogen-adsorption data were obtained for an Fe-Al₂O₃ ammonia catalyst. The results for a 50.4-g sample were:

Pressure, mm Hg	8	30	50	102	130	148	233	
Volume adsorbed, cm ³ (at 0°C and 1 atm)	103	116	130	148	159	163	188	
					258	330	442	480
					198	221	270	294
								316
								365

Estimate the surface area for this catalyst.

- 8-7. Ritter and Drake¹ give the true density of the solid material in an activated alumina particle as 3.675 g/cm³. The density of the particle determined by mercury displacement is 1.547. The surface area by adsorption measurement is 175 m²/g. From this information compute the pore volume per gram, the porosity of the particles, and the mean pore radius. The bulk density of a bed of the alumina particles in a 250-cm³ graduate is 0.81 g/cm³. What fraction of the total volume of the bed is void space between the particles and what fraction is void space within the particles?
- 8-8. Two samples of silica-alumina cracking catalysts have particle densities of 1.126 and 0.962 g/cm³, respectively, as determined by mercury displacement. The true density of the solid material in each case is 2.37 g/cm³. The surface area of the first sample is 467 m²/g and that of the second is 372 m²/g. Which sample has the larger mean pore radius?
- 8-9. Mercury porosimeter data are tabulated below for a 0.400-g sample of UO₂ pellet. At the beginning of the measurements (*p* = 1.77 psia) the mercury displaced by the sample was 0.125 cm³. At this low pressure no pores were penetrated. Data obtained with a pycnometer gave a true density of the solid phase of $\rho_s = 7.57$ g/cm³.

Calculate the total porosity of the pellet and the porosity due to pores of

¹H. L. Ritter and L. C. Drake, *Ind. Eng. Chem., Anal. Ed.*, 17, 787 (1945).

larger than 250 Å radius. Also plot the pore-volume distribution for the pores larger than 250 Å radius, using the coordinates of Fig. 8-7.

Pressure, psi	196	296	396	500	600	700	800	900
Mercury penetration, cm ³	0.002	0.004	0.008	0.014	0.020	0.026	0.032	0.038
	1,000	1,200	1,400	1,800	2,400	2,800	3,400	5,000
	0.044	0.052	0.057	0.062	0.066	0.066	0.067	0.068